Long-term culture of primary naïve T lymphocytes with HCV-core expressing lenti-virus

We constructed the HCV-core expressing lenti-virus to analyze the long-term culture of primary naïve T lymphocytes with the expression of HCV core protein. The efficiency of lenti-virus infection was 27.7±3% (average±standard deviation). In addition to IL1β and IL23, the IL6 and TGF-β1 cytokine conditions could remarkably induce the RORγt mRNA (Fig.4C). Moreover, significantly higher amounts of RORγt mRNA were detected in the HCV-core expressing T lymphocytes in comparison with the control groups (Fig. 4C)($p<0.05$).

Discussion

Autoimmune thyroiditis, systemic lupus erythematosus, idiopathic thrombocytopenic purpura, autoimmune hepatitis and rheumatoid arthritis etc. could be classified not only as HCV-related diseases but also as Th17-related autoimmune diseases[16-19,34–36]. In this study, we clearly demonstrated the relevance of lymphotropic HCV to autoimmune-related diseases including an important role of Th17 cells in CH-C patients. This study revealed two important mechanisms by which Th17 development is enhanced. In the first, the existence of lymphotropic HCV can result in the IL6 and TGF-β1 double high condition that can enhance Th17 development. Previously, Machida et al. described that HCV replication in B cells induced IL6 production from B cells[24]. In the second, the existence of HCV in naïve T cells can enhance Th17 development in the IL6 and TGF-β1 double high condition by enhancing STAT-3/RORγt signaling. Previously, we showed that lymphotropic HCV could suppress IFN-γ/STAT-1/T-bet signaling, which could contribute to the persistence of hepatitis C virus infection[1,4,13]. STAT-3 signaling could be enhanced by the suppression of STAT-1 signaling. However, the finding of our research was surprising. Therefore, we examined this phenomenon studiously and carefully. First, we found a novel genotype, 1b lymphotropic HCV strain (Ly-HCV), that could infect Raji and human primary lymphocytes. Although the infectivity of this strain was lower than that of SB-HCV[29], we could detect negative and positive strand RNA in naïve T lymphocytes with stimulation.

Therefore, we used two lymphotropic HCV strains to analyze the effect on Th17 development. Moreover, two kinds of expression experiments showed that HCV-Core could enhance the STAT-3/RORγt signaling, since the method of gene expression and the period of incubation might affect the result of T cell development. However, the results of our two kinds of experiments (plasmids and lenti-virus) consistently showed that the expression of HCV-core protein in T lymphocytes could enhance the Th17 development. Other groups previously reported that HCV-core protein could affect anergy-related genes and T cell responses by inducing spontaneous and alternating T-cell receptor-triggered Ca2+ oscillations[37,38]. Therefore, the expression of HCV-core protein in T lymphocyte might be important for the functional changes in T lymphocytes. Although our study confirmed that the replication of HCV in lymphocytes is important, there was a bystander effect by exosome produced from HCV-infected lymphocytes. Previously, our group reported that exosome could transport miRNA and proteins in the microenviroment[39,40]. This phenomenon could explain the significant effects of a low level of HCV infection in lymphocytes. Moreover, the naïve T lymphocyte is located upstream of Th17 development. Therefore, we should not underestimate the effect of a low-level of HCV replication in lymphocytes.

In conclusion, we report the detailed mechanism of Th17 development and HCV infection, which might be involved in the pathogenesis of autoimmune-related disease in CH-C patients (Fig S2). Recently, a novel therapy targeting STAT-3 signaling was reported[23,41,42]. We should consider the clinical use of such treatments for autoimmune-related diseases in CH-C patients.

Supporting Information

Figure S1 Phylogenetic trees constructed based on the nearly entire nucleotide sequence of HCV by using the unweighted pair group method with the arithmetic mean (Michener 1957). The tree includes the three genotype 1a isolates, forty 1b, one 1c, three 2a, two 2b, one 2c and one 3a, 3b, 6b, 7b, 9b, 10a, whose nucleotide sequence data were retrievable from the GenBank/EMBL/DDBJ database (A). Mapping to the consensus HCV genome sequence. For Ly-HCV 0183-4, 197,414 reads were mapped (Fig S1B). The coverage was 100.0%, and the average depth was 2092.1x. For Ly-HCV 0186-1, 410 reads were aligned. The coverage was 95.9%, and the average depth was 4.3× (B).
(TIFF)

Figure S2 The schema of Th17 induction in perihepatic lymph node of CH-C patient with lymphotropic HCV are shown.
(TIFF)

Table S1 Various kinds of cytokines conditions for in vitro analysis are shown in Table S1.
(DOC)

Acknowledgments

We are grateful to Prof. Ishii N who gave us valuable insight regarding NOG mice. We thank M. Tsuda, N. Koshita, M. Kikuchi and K. Kuroda for technical assistance. We also acknowledge the technical support of the Biomedical Research Core of Tohoku University Graduate School of Medicine.

Author Contributions

Conceived and designed the experiments: YK MN OK TK ML TS. Performed the experiments: YK MN OK KM RF TN KK EK KN. Analyzed the data: YK MN OK TN KN ML TS. Contributed reagents/materials/analysis tools: KM. Wrote the paper: YK MN TN ML TS.

References

1. Kondo Y, Ueno Y, Shimosegawa T (2012) Biological significance of HCV in various kinds of lymphoid cells. International journal of microbiology 2012: 647581.
2. Kondo Y, Ueno Y, Wakui Y, Ninomiya M, Kakazu E, et al. (2011) Rapid reduction of hepatitis C virus-Core protein in the peripheral blood improve the immunological response in chronic hepatitis C patients. Hepatol Res.
3. Kondo Y, Machida K, Liu HM, Ueno Y, Kobayashi K, et al. (2009) Hepatitis C virus infection of T cells inhibits proliferation and enhances fas-mediated apoptosis by down-regulating the expression of CD44 splicing variant 6. J Infect Dis 199: 726–736.
4. Kondo Y, Sung VM, Machida K, Liu M, Lai MM (2007) Hepatitis C virus infects T cells and affects interferon-gamma signaling in T cell lines. Virology 361: 161–173.
5. Machida K, Kondo Y, Huang JY, Chen YC, Cheng KT, et al. (2008) Hepatitis C virus (HCV)-induced immunoglobulin hypermutation reduces the affinity and neutralizing activities of antibodies against HCV envelope protein. J Virol 82: 6711–6720.
6. Simula MP, Caggiari L, Gloghini A, De Re V (2007) HCV-related immunocytoma and type II mixed cryoglobulinemia-associated autoantigens. Ann N Y Acad Sci 1110: 121–130.

7. Ito M, Masumi A, Mochida K, Kukihara H, Moriishi K, et al. (2010) Peripheral B cells may serve as a reservoir for persistent hepatitis C virus infection. J Innate Immun 2: 607–617.
8. Pal S, Sullivan DG, Kim S, Lai KK, Kae J, et al. (2006) Productive replication of hepatitis C virus in perihepatic lymph nodes in vivo: implications of HCV lymphotropism. Gastroenterology 130: 1107–1116.
9. Karavattathayyil SJ, Kalkeri G, Liu HJ, Gaglio P, Garry RF, et al. (2000) Detection of hepatitis C virus RNA sequences in B-cell non-Hodgkin lymphoma. Am J Clin Pathol 113: 391–398.
10. Ferri C, Zignego AL (2000) Relation between infection and autoimmunity in mixed cryoglobulinemia. Curr Opin Rheumatol 12: 53–60.
11. Mariette X (1999) Lymphomas in patients with Sjogren's syndrome: review of *the literature and physiopathologic hypothesis. Leuk Lymphoma* 33: 93–99.
12. Mizukawa Y, Shiohara T (2000) Virus-induced immune dysregulation as a triggering factor for the development of drug rashes and autoimmune diseases: with emphasis on EB virus, human herpesvirus 6 and hepatitis C virus. J Dermatol Sci 22: 169–180.
13. Kondo Y, Ueno Y, Kakazu E, Kobayashi K, Shiina M, et al. (2011) Lymphotropic HCV strain can infect human primary naive CD4+ cells and affect their proliferation and IFN-gamma secretion activity. J Gastroenterol 46: 232–241.
14. MacParland SA, Pham TN, Gujar SA, Michalak TI (2006) De novo infection and propagation of wild-type Hepatitis C virus in human T lymphocytes in vitro. J Gen Virol 87: 3577–3586.
15. Hu Y, Shahidi A, Park S, Guilfoyle D, Hirshfield I (2003) Detection of extrahepatic hepatitis C virus replication by a novel, highly sensitive, single-tube nested polymerase chain reaction. Am J Clin Pathol 119: 95–100.
16. Bassiouny DA, Shaker O (2011) Role of interleukin-17 in the pathogenesis of vitiligo. Clinical and experimental dermatology 36: 292–297.
17. Horie I, Abiru N, Saitoh O, Ichikawa T, Iwakura Y, et al. (2011) Distinct role of T helper Type 17 immune response for Graves' hyperthyroidism in mice with different genetic backgrounds. Autoimmunity 44: 159–165.
18. Horie I, Abiru N, Sakamoto H, Iwakura Y, Nagayama Y (2011) Induction of autoimmune thyroiditis by depletion of CD4+CD25+ regulatory T cells in thyroiditis-resistant IL-17, but not interferon-gamma receptor, knockout nonobese diabetic-H2h4 mice. Endocrinology 152: 4448–4454.
19. Zhao L, Tang Y, You Z, Wang Q, Liang S, et al. (2011) Interleukin-17 contributes to the pathogenesis of autoimmune hepatitis through inducing hepatic interleukin-6 expression. PLoS One 6: e18909.
20. Ivanov, II, McKenzie BS, Zhou L, Tadokoro CE, Lepelley A, et al. (2006) The orphan nuclear receptor RORgammat directs the differentiation program of proinflammatory IL-17+ T helper cells. Cell 126: 1121–1133.
21. Harris TJ, Grosso JF, Yen HR, Xin H, Kortylewski M, et al. (2007) Cutting edge: An in vivo requirement for STAT3 signaling in TH17 development and TH17-dependent autoimmunity. Journal of immunology 179: 4313–4317.
22. Seddighzadeh M, Gonzalez A, Ding B, Ferreiro-Iglesias A, Gomez-Reino JJ, et al. (2012) Variants Within STAT Genes Reveal Association with Anticitrullinated Protein Antibody-negative Rheumatoid Arthritis in 2 European Populations. The Journal of rheumatology 39: 1509–1516.
23. Yu CR, Lee YS, Mahdi RM, Surendran N, Egwuagu CE (2012) Therapeutic targeting of STAT3 (signal transducers and activators of transcription 3) pathway inhibits experimental autoimmune uveitis. PLoS One 7: e29742.
24. Machida K, Cheng KT, Sung VM, Levine AM, Foung S, et al. (2006) Hepatitis C virus induces toll-like receptor 4 expression, leading to enhanced production of beta interferon and interleukin-6. J Virol 80: 866–874.
25. Korn T, Bettelli E, Oukka M, Kuchroo VK (2009) IL-17 and Th17 Cells. Annual review of immunology 27: 485–517.
26. Kondo Y, Iwata T, Haga T, Kimura O, Ninomiya M, et al. (2013) Eradication of hepatitis C virus could improve immunological status and pyoderma gangrenosum-like lesions. Hepatology research: the official journal of the Japan Society of Hepatology.
27. Negro F, Krawczynski K, Quadri R, Rubbia-Brandt L, Mondelli M, et al. (1999) Detection of genomic- and minus-strand of hepatitis C virus RNA in the liver of chronic hepatitis C patients by strand-specific semiquantitative reverse-transcriptase polymerase chain reaction. Hepatology 29: 536–542.
28. Hu Y, Shahidi A, Park S, Guilfoyle D, Hirshfield I (2003) Detection of extrahepatic hepatitis C virus replication by a novel, highly sensitive, single-tube nested polymerase chain reaction. American journal of clinical pathology 119: 95–100.
29. Sung VM, Shimodaira S, Doughty AL, Picchio GR, Can H, et al. (2003) Establishment of B-cell lymphoma cell lines persistently infected with hepatitis C virus in vivo and in vitro: the apoptotic effects of virus infection. J Virol 77: 2134–2146.
30. Tuomela S, Salo V, Tripathi SK, Chen Z, Laurila K, et al. (2012) Identification of early gene expression changes during human Th17 cell differentiation. Blood 119: e151–160.
31. Takeuchi K, Kubo Y, Boonmar S, Watanabe Y, Katayama T, et al. (1990) *Nucleotide sequence of core and envelope genes of the hepatitis C virus genome* derived directly from human healthy carriers. Nucleic acids research 18: 4626.
32. Zhou J, Yu Z, Zhao S, Hu L, Zheng J, et al. (2009) Lentivirus-based DsRed-2-transfected pancreatic cancer cells for deep in vivo imaging of metastatic disease. The Journal of surgical research 157: 63–70.
33. Shiokawa M, Takahashi T, Murakami A, Kita S, Ito M, et al. (2010) In vivo assay of human NK-dependent ADCC using NOD/SCID/gammac(null) (NOG) mice. Biochemical and biophysical research communications 399: 733–737.
34. Chen XQ, Yu YC, Deng HH, Sun JZ, Dai Z, et al. (2010) Plasma IL-17A is increased in new-onset SLE patients and associated with disease activity. J Clin Immunol 30: 221–225.
35. Pan HF, Leng RX, Feng CC, Li XP, Chen GM, et al. (2012) Expression profiles of Th17 pathway related genes in human systemic lupus erythematosus. Mol Biol Rep.
36. Hu Y, Li H, Zhang L, Shan B, Xu X, et al. (2012) Elevated profiles of Th22 cells and correlations with Th17 cells in patients with immune thrombocytopenia. Hum Immunol 73: 629–635.
37. Bergqvist A, Sundstrom S, Dimberg LY, Gylfe E, Masucci MG (2003) The hepatitis C virus core protein modulates T cell responses by inducing spontaneous and altering T-cell receptor-triggered Ca2+ oscillations. J Biol Chem 278: 18877–18883.
38. Dominguez-Villar M, Munoz-Suano A, Anaya-Baz B, Aguilar S, Novalbos JP, et al. (2007) Hepatitis C virus core protein up-regulates anergy-related genes and a new set of genes, which affects T cell homeostasis. J Leukoc Biol 82: 1301–1310.
39. Kogure T, Lin WL, Yan IK, Braconi C, Patel T (2011) Intercellular nanovesicle-mediated microRNA transfer: a mechanism of environmental modulation of hepatocellular cancer cell growth. Hepatology 54: 1237–1248.
40. Tamai K, Shiina M, Tanaka N, Nakano T, Yamamoto A, et al. (2012) Regulation of hepatitis C virus secretion by the Hrs-dependent exosomal pathway. Virology 422: 377–385.
41. Stump KL, Lu LD, Dobrzanski P, Serdikoff C, Gingrich DE, et al. (2011) A highly selective, orally active inhibitor of Janus kinase 2, CEP-33779, ablates disease in two mouse models of rheumatoid arthritis. Arthritis research & therapy 13: R68.
42. Zhang X, Yue P, Page BD, Li T, Zhao W, et al. (2012) Orally bioavailable small-molecule inhibitor of transcription factor Stat3 regresses human breast and lung cancer xenografts. Proc Natl Acad Sci U S A 109: 9623–9628.

Available online at www.sciencedirect.com

ScienceDirect

Neuromuscular Disorders 24 (2014) 1068–1072

www.elsevier.com/locate/nmd

Case report

GNE myopathy associated with congenital thrombocytopenia: A report of two siblings

Rumiko Izumi [a,b], Tetsuya Niihori [a], Naoki Suzuki [b], Yoji Sasahara [c], Takeshi Rikiishi [c], Ayumi Nishiyama [a,b], Shuhei Nishiyama [b], Kaoru Endo [b], Masaaki Kato [b], Hitoshi Warita [b], Hidehiko Konno [d], Toshiaki Takahashi [d], Maki Tateyama [b], Takeshi Nagashima [e], Ryo Funayama [e], Keiko Nakayama [e], Shigeo Kure [c], Yoichi Matsubara [a], Yoko Aoki [a], Masashi Aoki [b,*]

[a] *Department of Medical Genetics, Tohoku University School of Medicine, Sendai, Japan*
[b] *Department of Neurology, Tohoku University School of Medicine, Sendai, Japan*
[c] *Department of Pediatrics, Tohoku University School of Medicine, Sendai, Japan*
[d] *Department of Neurology and Division of Clinical Research, Sendai Nishitaga National Hospital, Sendai, Japan*
[e] *Division of Cell Proliferation, United Centers for Advanced Research and Translational Medicine, Tohoku University Graduate School of Medicine, Sendai, Japan*

Received 2 May 2014; received in revised form 13 July 2014; accepted 30 July 2014

Abstract

GNE myopathy is an autosomal recessive muscular disorder caused by mutations in the gene encoding the key enzyme in sialic acid biosynthesis, UDP-N-acetylglucosamine 2-epimerase/N-acetylmannosamine kinase (GNE/MNK). Here, we report two siblings with myopathy with rimmed vacuoles and congenital thrombocytopenia who harbored two compound heterozygous *GNE* mutations, p.V603L and p.G739S. Thrombocytopenia, which is characterized by shortened platelet lifetime rather than ineffective thrombopoiesis, has been observed since infancy. We performed exome sequencing and array CGH to identify the underlying genetic etiology of thrombocytopenia. No pathogenic variants were detected among the known causative genes of recessively inherited thrombocytopenia; yet, candidate variants in two genes that followed an autosomal recessive mode of inheritance, including previously identified *GNE* mutations, were detected. Alternatively, it is possible that the decreased activity of GNE/MNK itself, which would lead to decreased sialic content in platelets, is associated with thrombocytopenia in these patients. Further investigations are required to clarify the association between *GNE* myopathy and the pathogenesis of thrombocytopenia.

Keywords: *GNE*; Distal myopathy with rimmed vacuoles; Sialic acid; UDP-N-acetylglucosamine 2-epimerase/N-acetylmannosamine kinase; Thrombocytopenia; Exome sequencing

1. Introduction

GNE myopathy is a group of autosomal recessive muscular disorders caused by mutations in *GNE*, which encodes the key enzyme of sialic acid biosynthesis, UDP-N-acetylglucosamine 2-epimerase/N-acetylmannosamine kinase (GNE/MNK). This enzyme initiates and regulates the biosynthesis of

* Corresponding author. Address: Department of Neurology, Tohoku University School of Medicine, 1-1 Seiryo-machi, Aoba-ku, Sendai 980-8574, Japan. Tel.: +81 22 717 7189; fax: +81 22 717 7192.
E-mail address: aokim@med.tohoku.ac.jp (M. Aoki).

http://dx.doi.org/10.1016/j.nmd.2014.07.008
0960-8966/

N-acetylneuraminic acid [1], a substrate for sialylation. *GNE* mutations have been identified in both hereditary inclusion body myopathy [2,3] and Nonaka myopathy, which is also called distal myopathy with rimmed vacuoles (DMRV; MIM#605820) [4,5]. Since these conditions have been confirmed to be the same, they are now generically referred to as *GNE* myopathy.

Here, we report two siblings with compound heterozygous *GNE* mutations who manifested a myopathy with rimmed vacuoles associated with thrombocytopenia. The phenotypes of patients with *GNE* myopathy are variable; however, hematological complications are rare. To identify the underlying genetic etiology of thrombocytopenia in these siblings, we performed exome sequencing and array CGH. The possibility of a genetic defect in sialic acid biosynthesis as a cause of thrombocytopenia is also discussed.

2. Case report

2.1. Patients

The siblings described in this study are of Japanese ancestry and the only offspring of nonconsanguineous parents. Their parents and other family members have no medical history of hematological or neuromuscular disorders.

Patient 1 is a 32-year-old man and the thrombocytopenia was detected during treatment for neonatal jaundice. His thrombocytopenia persisted, with a platelet count ranging from 1.7×10^9/L to 16.2×10^9/L. He had no other congenital abnormalities or developmental delays. Megakaryocytes in the bone marrow, observed at the age of 8 years, were morphologically normal and increased in number to 281/mm^3, and his nuclear cell count was normal at 37.4×10^4/mm^3. The size of his peripheral blood platelets was normal to large, and the mean platelet volume was 10–11 fl. Platelet-associated IgG (PAIgG) was elevated (207.3 ng/10^7 cells), and von Willebrand factor activity was within the normal range. At the age of 7 years, proteinuria and hematuria were detected. Kidney biopsy revealed atypical membranoproliferative glomerulonephritis, which later progressed to chronic renal failure requiring periodic dialysis therapy. He had a waddling gait that began in middle adolescence and muscle weakness that gradually progressed, particularly in the proximal lower limbs. Neurological examination at the age of 20 years showed proximal muscle weakness, particularly in the neck flexor and iliopsoas. His serum creatine kinase levels ranged from 300 to 600 IU/L. Muscle biopsy specimens taken from the rectus femoris of Pathological findings of the rectus femoris showed increased rimmed vacuoles in approximately 1% of myofibers, located predominantly in atrophic fibers. Necrotic and regenerating fibers were rare, and no inflammatory cellular infiltration was observed. Mutation analysis of *GNE* identified the following two missense mutations: c.1807G > C (NM_001128227); p.V603L (NP_001121699) and c.2215G > A; p.G739S, both of which have been reported previously as causes of DMRV [6,7]. Parental analysis confirmed that he was a compound heterozygote for these mutations. He has been wheelchair-bound since the age of 24 years. From the age of 22 years, he has had mildly decreased cardiac function accompanied by mitral insufficiency, but his respiratory system has remained fully functional so far.

Patient 2, a 29-year-old woman, is the younger sister of Patient 1. Her thrombocytopenia was incidentally found at the age of 2 years while undergoing treatment for pneumonia. Her thrombocytopenia persisted, with a platelet count ranging from 1.1×10^9/L to 9.0×10^9/L. This induced intermittent nasal bleeding. Megakaryocytes in her bone marrow, observed at the age of 5 years, were normal in number and morphology. Her platelets were normal to large in size, with a mean volume of 10–13 fl (Fig. 1), and her PAIgG was elevated (119 ng/10^7 cells). At the age of 18 years, she exhibited proximal muscle weakness accompanied by difficulties in standing and lifting her arms. At the age of 23 years, her muscle strength decreased in the neck and overall proximal muscles, and she developed a waddling gait. Muscle imaging showed remarkable atrophy in the paraspinal muscles and moderate patchy atrophy in the adductor magnus, soleus and tibialis posterior muscles. Her serum creatine kinase level was elevated (360 IU/L). Pathological findings of the biceps brachii were essentially similar to those of Patient 1 (Fig. 2). Genetic testing for *GNE* indicated that she also harbored the p.V603L and p.G739S mutations. Systemic examination revealed moderate splenomegaly, but normal cardiorespiratory and renal functions were maintained. She is still able to walk independently with a simple walking aid.

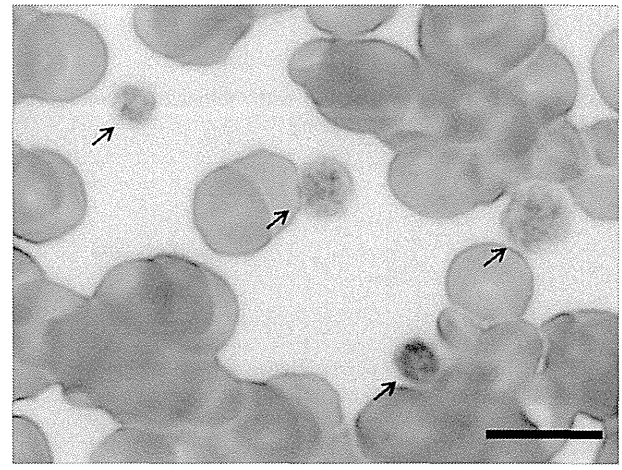

Fig. 1. Morphology of peripheral blood platelets a blood smear from Patient 2 showing morphologically normal platelets (arrow). The size of platelets was normal to large. Bars = 10 μm.

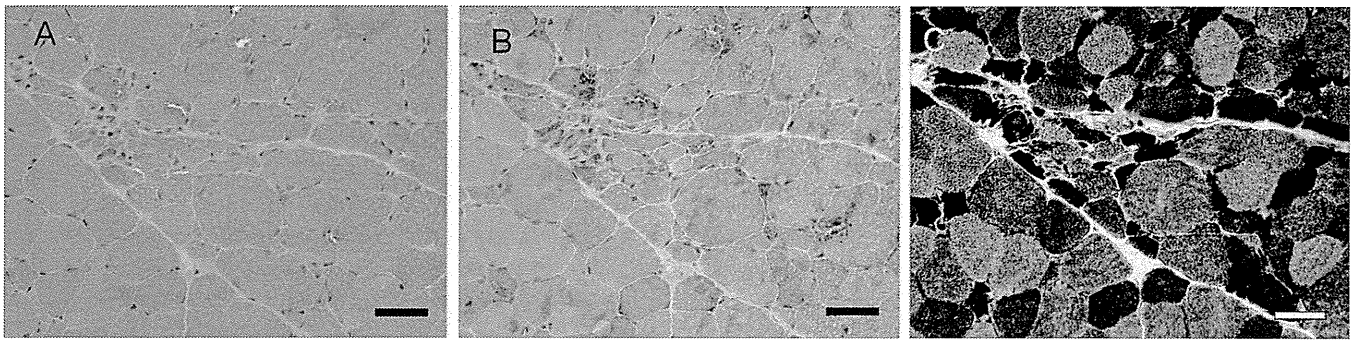

Fig. 2. Pathology of the muscle biopsy specimens hematoxylin-eosin (A), Gomori-trichrome (B) and NADH-tetrazolium reductase (C) staining of the muscle biopsy sample from the biceps brachii of patient 2 are shown. Atrophic fibers were clustering into small groups, including both type 1 and type 2 myofibers. Several rimmed vacuoles were scattered around them predominantly located on atrophic fibers. NADH-tetrazolium reductase staining showed an almost normal myofibrillar network. Bars = 50 μm.

2.2. Exome sequencing and array CGH

Exome sequencing and array CGH were performed on peripheral blood samples from the siblings and their parents to determine the genetic cause of thrombocytopenia. This study was approved by the Ethics Committee of the Tohoku University School of Medicine, and all individuals gave their informed consent prior to their inclusion in the study.

2.2.1. Exome sequencing

The detailed methods regarding exome sequencing were described in our previous report [8]. After excluding synonymous SNVs, we used the 1000 Genomes to filter out frequent variants. Three pairs of rare variants (i.e., not present or <1% allele frequency according to the 1000 Genomes), which were segregated in an autosomal recessive mode, were identified in *CPEB2, FLNB* and *GNE* (Supplementary Tables 1 and 2). The mutation in *CPEB2* was present with 13.7% allele frequency and with 1.9% in homozygous state according to Human Genetic Variation Database (http://www.genome.med.kyoto-u.ac.jp/SnpDB/), thus seemed less pathogenic. Exome sequencing enabled comprehensive screening for the causative genes of recessively inherited thrombocytopenia with coverage of 95% of all targeted regions at ⩾20-fold and we did not detect any novel or rare homozygous or compound heterozygous mutations among these genes (Supplementary Table 3).

2.2.2. Array CGH

Array CGH was performed using the Agilent SurePrint G3 Human Custom CNV 2 × 400 K microarray for all individuals, and it revealed three regions with recessively inherited deletions of genomic copy number (Supplementary Table 4). None of the genes in or around these deleted regions have been previously reported as being responsible for myopathy or thrombocytopenia.

3. Discussion

In this study, we described two siblings harboring two compound heterozygous *GNE* mutations, p.V603L and p.G739S, who were diagnosed with myopathy with rimmed vacuoles associated with congenital thrombocytopenia.

The pathogenesis of thrombocytopenia involves various congenital or acquired disorders. Familial occurrence of thrombocytopenia in the neonatal period and infancy strongly suggests the involvement of a genetic defect. Hereditary thrombocytopenia is extremely heterogeneous in terms of the gene mutations involved, although the genetic background contributing to this condition remains to be elucidated [9]. Exome sequencing identified substantially two pairs of rare compound heterozygous variants in *FLNB* and *GNE*, which cosegregated in a recessive mode (Supplementary Table 2). The one encoding filamin b is highly homologous to the gene encoding filamin a (*FLNA*), which is located on chromosome Xq28. Although a missense mutation in *FLNA* has been reported as a cause of nonsyndromic thrombocytopenia [10], the pathogenicity of *FLNB* variants in this family remains unknown.

GNE mutations result in the loss of its enzymatic activity and failure to catalyze the initial two steps in sialic acid biosynthesis, leading to decreased sialic acid content in the organs [11]. This hyposialylation and abnormal glycosylation in muscles have been thought to contribute to the pathogenesis of *GNE* myopathy [12]. In this context, hyposialylation caused by *GNE* mutations may be a common defect in muscles and platelets. Sialic acid is known to play significant roles in platelet function, is located in the platelet membrane, and forms a part of glycosylation. Several groups have shown that platelets deficient in sialylation are easily removed from circulation, resulting in shortened circulation lifetimes and thrombocytopenia [13–15]. Decreased sialic acid content in platelets has also been reported in

infection-induced thrombosis [16], and hepatic cirrhosis [17]. These findings suggest that sialic acid is an essential molecule for the stabilization of circulating platelets, and hyposialylation of platelets can be a general risk factor for thrombocytopenia.

Recently, another group reported a family with distal myopathy with rimmed vacuoles associated with thrombocytopenia [18]; they suggested that two novel specific *GNE* mutations identified in the affected siblings, p.Y217H and p.D515Qfs*2, may have led to thrombocytopenia. In contrast, the p.V603L mutation identified in our cases is the most common among the Japanese population [5,6], while the p.G739S mutation occurs rather infrequently [7,19,20]. However, it still remains unknown whether thrombocytopenia is associated with *GNE* myopathy in general or rather with these specific *GNE* mutations. Careful observation of the hematologic features in other patients with *GNE* myopathy will reveal whether *GNE* myopathy is frequently associated with thrombocytopenia.

The reason for elevated PAIgG observed in our cases remains unknown. PAIgG is elevated in patients with immune and nonimmune thrombocytopenia, and its pathogenic effect has not been fully established [21]. Dysregulation of immune system has not been reported in individuals with *GNE* myopathy. However, a past report showed that the removal of sialic acid from platelet membranes and an increase in PAIgG were observed in baboons, suggesting that the loss of sialic acid may have exposed senescent cell antigens [14]. Further analysis will be necessary to clarify the mechanism of elevated PAIgG in our cases.

Patient 1 manifested atypical membranoproliferative glomerulonephritis with proteinuria and hematuria. The renal pathology including diffuse thickening of the glomerular basement membrane with the appearance of double contours is similar to those reported in *GNE* mutant mice [22,23], suggesting his nephritic phenotype is associated with *GNE* mutations. Membranoproliferative glomerulonephritis is sometimes accompanied by thrombocytopenia from platelet consumption. However the early onset of thrombocytopenia and patient 2's maintained renal function mean the mechanism of their thrombocytopenia is independent of renal pathology.

In conclusion, we described two siblings with the *GNE* mutations, p.V603L and p.G739S, who manifested both myopathy and thrombocytopenia. Genetic alterations to known causative genes for autosomal recessive thrombocytopenia were not identified by exome sequencing. Therefore, we could not conclude whether the rare candidate variants detected by exome sequencing or the deletions identified by array CGH had any pathogenic role in thrombocytopenia observed in our cases. Hence, further investigations are required to clarify the possible association between *GNE* myopathy and the pathogenesis of thrombocytopenia observed in these patients.

Acknowledgments

We thank the patients and their parents. We are also grateful to Drs. Shigeru Tsuchiya and Madoka Mori for their fruitful discussion and Yoko Tateda, Kumi Kato, Naoko Shimakura, Risa Ando, Riyo Takahashi, Miyuki Tsuda, Makiko Nakagawa, Mami Kikuchi, and Kiyotaka Kuroda for their technical assistance. We also acknowledge the support of the Biomedical Research Core of Tohoku University Graduate School of Medicine. This work was supported by a grant for Research on Applying Health Technology provided by the Ministry of Health, Labor and Welfare to YM and an Intramural Research Grant (23-5) for Neurological and Psychiatric Disorders of NCNP, JSPS KAKENHI (Grant Number 24659421) and Research on Measures for Intractable Diseases from the Japanese Ministry of Health, Labor and Welfare to MA.

Appendix A. Supplementary data

Supplementary data associated with this article can be found, in the online version, at http://dx.doi.org/10.1016/j.nmd.2014.07.008.

References

[1] Stasche R, Hinderlich S, Weise C, et al. A bifunctional enzyme catalyzes the first two steps in N-acetylneuraminic acid biosynthesis of rat liver. Molecular cloning and functional expression of UDP-N-acetyl-glucosamine 2-epimerase/N-acetylmannosamine kinase. J Biol Chem 1997;272:24319–24.

[2] Argov Z, Yarom R. "Rimmed vacuole myopathy" sparing the quadriceps. A unique disorder in Iranian Jews. J Neurol Sci 1984;64:33–43.

[3] Eisenberg I, Avidan N, Potikha T, et al. The UDP-N-acetylglucosamine 2-epimerase/N-acetylmannosamine kinase gene is mutated in recessive hereditary inclusion body myopathy. Nat Genet 2001;29:83–7.

[4] Nonaka I, Sunohara N, Ishiura S, Satoyoshi E. Familial distal myopathy with rimmed vacuole and lamellar (myeloid) body formation. J Neurol Sci 1981;51:141–55.

[5] Nishino I, Noguchi S, Murayama K, et al. Distal myopathy with rimmed vacuoles is allelic to hereditary inclusion body myopathy. Neurology 2002;59:1689–93.

[6] Tomimitsu H, Ishikawa K, Shimizu J, et al. Distal myopathy with rimmed vacuoles: novel mutations in the *GNE* gene. Neurology 2002;59:451–4.

[7] Tomimitsu H, Shimizu J, Ishikawa K, et al. Distal myopathy with rimmed vacuoles (DMRV): new *GNE* mutations and splice variant. Neurology 2004;62:1607–10.

[8] Izumi R, Niihori T, Aoki Y, et al. Exome sequencing identifies a novel TTN mutation in a family with hereditary myopathy with early respiratory failure. J Hum Genet 2013;58:259–66.

[9] Balduini CL, Savoia A. Genetics of familial forms of thrombocytopenia. Hum Genet 2012;131:1821–32.

[10] Nurden P, Debili N, Coupry I, et al. Thrombocytopenia resulting from mutations in filamin A can be expressed as an isolated syndrome. Blood 2011;118:5928–37.

[11] Malicdan MC, Noguchi S, Nonaka I, Hayashi YK, Nishino I. A GNE knockout mouse expressing human V572L mutation develops

features similar to distal myopathy with rimmed vacuoles or hereditary inclusion body myopathy. Hum Mol Genet 2007;16:115–28.
[12] Noguchi S, Keira Y, Murayama K, et al. Reduction of UDP-N-acetylglucosamine 2-epimerase/N-acetylmannosamine kinase activity and sialylation in distal myopathy with rimmed vacuoles. J Biol Chem 2004;279:11402–7.
[13] Greenberg J, Packham MA, Cazenave JP, Reimers HJ, Mustard JF. Effects on platelet function of removal of platelet sialic acid by neuraminidase. Lab Invest 1975;32:476–84.
[14] Kotze HF, van Wyk V, Badenhorst PN, et al. Influence of platelet membrane sialic acid and platelet-associated IgG on ageing and sequestration of blood platelets in baboons. Thromb Haemost 1993;70:676–80.
[15] Sorensen AL, Rumjantseva V, Nayeb-Hashemi S, et al. Role of sialic acid for platelet life span: exposure of beta-galactose results in the rapid clearance of platelets from the circulation by asialoglycoprotein receptor-expressing liver macrophages and hepatocytes. Blood 2009;114:1645–54.
[16] Tribulatti MV, Mucci J, Van Rooijen N, Leguizamon MS, Campetella O. The trans-sialidase from *Trypanosoma cruzi* induces thrombocytopenia during acute Chagas' disease by reducing the platelet sialic acid contents. Infect Immun 2005;73:201–7.
[17] Watanabe Y. The mechanism of the thrombocytopenia in patients with hepatic cirrhosis. J Jpn Soc Gastroenterol 1981;78:1216–25 (Japanese).
[18] Zhen C, Guo F, Fang X, Liu Y, Wang X. A family with distal myopathy with rimmed vacuoles associated with thrombocytopenia. Neurol Sci 2014.
[19] Kurochkina N, Yardeni T, Huizing M. Molecular modeling of the bifunctional enzyme UDP-GlcNAc 2-epimerase/ManNAc kinase and predictions of structural effects of mutations associated with HIBM and sialuria. Glycobiology 2010;20:322–37.
[20] Mori-Yoshimura M, Monma K, Suzuki N, et al. Heterozygous UDP-GlcNAc 2-epimerase and N-acetylmannosamine kinase domain mutations in the GNE gene result in a less severe GNE myopathy phenotype compared to homozygous N-acetylmannosamine kinase domain mutations. J Neurol Sci 2012;318:100–5.
[21] McMillan R. Autoantibodies and autoantigens in chronic immune thrombocytopenic purpura. Semin Hematol 2000;37:239–48.
[22] Ito M, Sugihara K, Asaka T, et al. Glycoprotein hyposialylation gives rise to a nephrotic-like syndrome that is prevented by sialic acid administration in GNE V572L point-mutant mice. PLoS One 2012;7:e29873.
[23] Galeano B, Klootwijk R, Manoli I, et al. Mutation in the key enzyme of sialic acid biosynthesis causes severe glomerular proteinuria and is rescued by N-acetylmannosamine. J Clin Invest 2007;117:1585–94.

Article

Molecular Cell

CRL4^{VprBP} E3 Ligase Promotes Monoubiquitylation and Chromatin Binding of TET Dioxygenases

Graphical Abstract

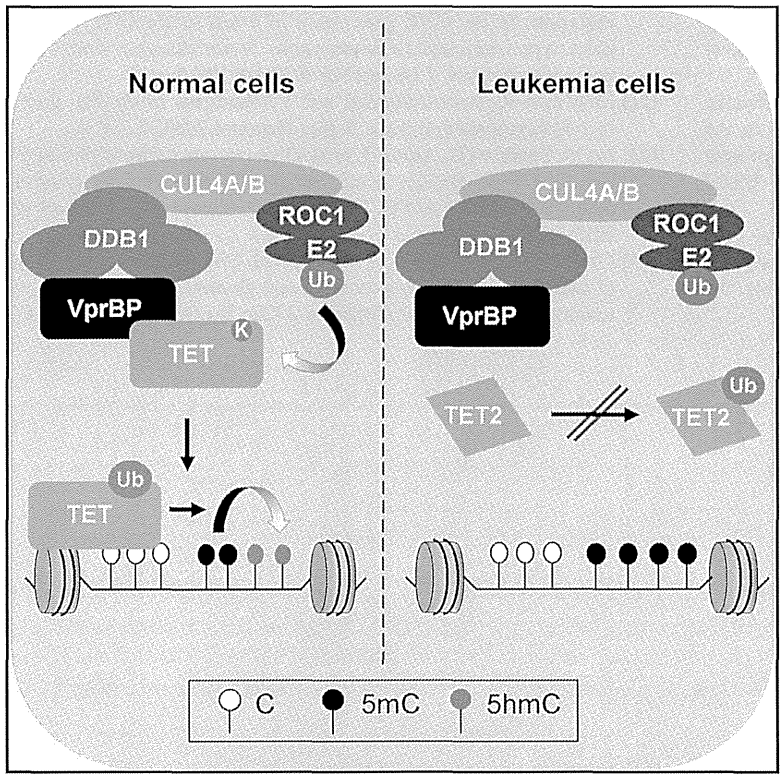

Authors

Tadashi Nakagawa, Lei Lv, ..., Xian Chen, Yue Xiong

Correspondence

yxiong@email.unc.edu

In Brief

The TET family of DNA dioxygenases regulates development and cell reprogramming and suppresses hematopoietic malignancy. Nakagawa et al. show that VprBP promotes TET monoubiquitylation which is required for its binding to chromatin. Deletion of VprBP abrogates paternal DNA hydroxymethylation in zygotes, and recurrent leukemia mutations in TET2 disrupt VprBP-catalyzed monoubiquitylation.

Highlights

- VprBP promotes TET monoubiquitylation on a conserved lysine
- VprBP is essential for zygotic paternal chromosome hydroxymethylation
- Monoubiquitylation promotes TET binding to DNA
- Recurrent leukemia mutations in TET2 disrupt VprBP-catalyzed monoubiquitylation

Nakagawa et al., 2015, Molecular Cell 57, 247–260
January 22, 2015
http://dx.doi.org/10.1016/j.molcel.2014.12.002

CellPress

Molecular Cell
Article

CRL4^{VprBP} E3 Ligase Promotes Monoubiquitylation and Chromatin Binding of TET Dioxygenases

Tadashi Nakagawa,[1,5] Lei Lv,[1,5] Makiko Nakagawa,[1] Yanbao Yu,[2] Chao Yu,[3] Ana C. D'Alessio,[1] Keiko Nakayama,[4] Heng-Yu Fan,[3] Xian Chen,[2] and Yue Xiong[1,2,*]
[1]Lineberger Comprehensive Cancer Center
[2]Department of Biochemistry and Biophysics
University of North Carolina at Chapel Hill, NC 27599, USA
[3]Life Sciences Institute, Zhejiang University, Hangzhou 310058, China
[4]Division of Cell Proliferation, ART, Graduate School of Medicine, Tohoku University, Sendai 980-8575, Japan
[5]Co-first authors
*Correspondence: yxiong@email.unc.edu
http://dx.doi.org/10.1016/j.molcel.2014.12.002

SUMMARY

DNA methylation at the C-5 position of cytosine (5mC) regulates gene expression and plays pivotal roles in various biological processes. The TET dioxygenases catalyze iterative oxidation of 5mC, leading to eventual demethylation. Inactivation of TET enzymes causes multistage developmental defects, impaired cell reprogramming, and hematopoietic malignancies. However, little is known about how TET activity is regulated. Here we show that all three TET proteins bind to VprBP and are monoubiquitylated by the VprBP-DDB1-CUL4-ROC1 E3 ubiquitin ligase (CRL4^{VprBP}) on a highly conserved lysine residue. Deletion of *VprBP* in oocytes abrogated paternal DNA hydroxymethylation in zygotes. VprBP-mediated monoubiquitylation promotes TET binding to chromatin. Multiple recurrent TET2-inactivating mutations derived from leukemia target either the monoubiquitylation site (K1299) or residues essential for VprBP binding. Cumulatively, our data demonstrate that CRL4^{VprBP} is a critical regulator of TET dioxygenases during development and in tumor suppression.

INTRODUCTION

5-methylcytosine (5mC) is a genomic modification that negatively regulates gene expression and is essential for diverse biological processes (Li, 2002; Wu and Zhang, 2014). 5mC patterning is established by DNA methyltransferase (DNMT) 3 and is maintained by DNMT1, which methylates newly replicated DNA (Goll and Bestor, 2005). Once considered irreversible, the recent identification of the TET family of proteins (TET1, TET2, and TET3 in mammalian cells) has changed our view of 5mC stability (Tahiliani et al., 2009; Ito et al., 2010). TET proteins are α-ketoglutarate (α-KG)- and Fe(II)-dependent dioxygenases that catalyze three steps of iterative oxidation, first converting 5mC to 5-hydroxymethyl cytosine (5hmC), then 5hmC to 5-formyl cytosine (5fC), and finally 5fC to 5-carboxy cytosine (5caC). 5caC can be removed by DNA glycosylase TDG, resulting in 5-unmodified cytosine (He et al., 2011; Ito et al., 2011). Besides being an intermediate in demethylation, emerging data indicate that 5hmC is recognized by several chromatin factors and may directly contribute to gene regulation (Mellén et al., 2012; Yildirim et al., 2011).

Conditional zygotic deletion of *Tet3* blocks paternal-genome conversion of 5mC into 5hmC and results in multiple developmental defects, supporting a critical developmental role for TET enzymes (Gu et al., 2011). Tet1 depletion results in defective DNA demethylation in primordial germ cells and decreased expression of a subset of meiotic genes, leading to reduced female germ cells and fertility (Yamaguchi et al., 2012). During induced pluripotent stem cell (iPSC) reprogramming, TET1 and TET2 promote 5mC-to-5hmC conversion to facilitate imprint erasure and establish pluripotency in somatic cells (Costa et al., 2013; Doege et al., 2012; Piccolo et al., 2013). Pathologically, the *TET2* gene is frequently mutated in human hematopoietic malignancies of both myeloid, in particular acute myeloid leukemia (AML, ~15%–20%), and lymphoid lineages, such as angioimmunoblastic T cell lymphoma (AITL, ~30%– 40%) (Delhommeau et al., 2009; Quivoron et al., 2011; Tefferi et al., 2009). While the biological function and catalytic mechanism of TET enzymes are extensively investigated, little is known about their regulation.

The covalent attachment of ubiquitin to a substrate protein (ubiquitylation) is involved in most cellular processes (Glickman and Ciechanover, 2002). Ubiquitylation proceeds through sequential reactions promoted by a ubiquitin-activating enzyme (E1), a ubiquitin-conjugating enzyme (E2), and finally a ubiquitin ligase (E3) that binds substrates and determines specificity. Substrate modification with either a single ubiquitin or various lengths and linkages of ubiquitin chains enables substrate recognition by distinct ubiquitin-binding proteins, leading to specific biochemical consequences including degradation, translocation, and recruitment of other proteins. Cullin proteins, which

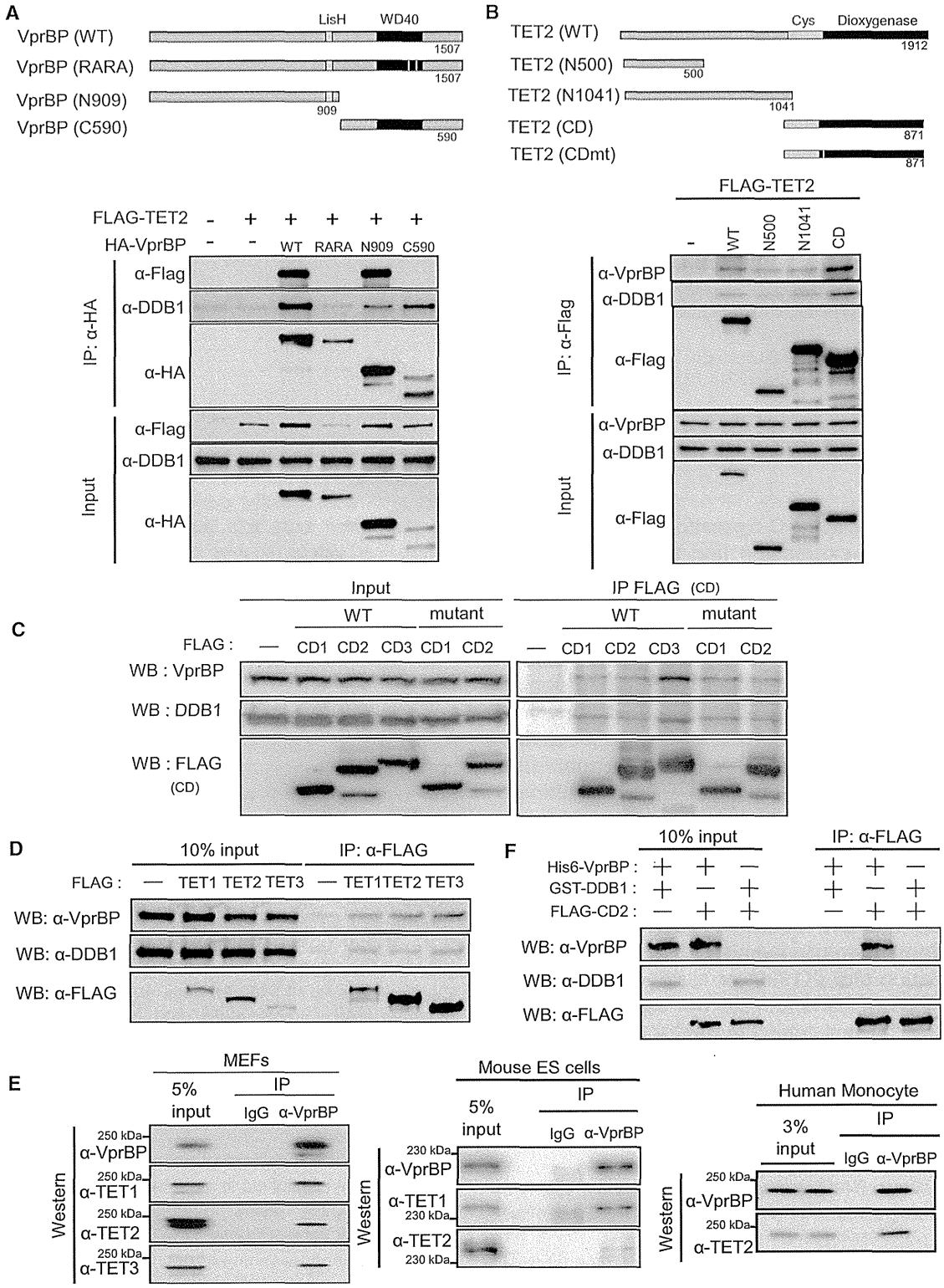

Figure 1. VprBP Binds to TET Family Proteins

(A) (Top) Domain structure of human VprBP. (Bottom) 293T cells were transiently transfected with expression vectors for FLAG-TET2 and a series of HA-VprBP fragments. Cell lysates were subjected to IP with an HA antibody, followed by western blot (WB).

(B) (Top) Domain structure of mouse TET2. (Bottom) 293T cells were transiently transfected with expression vectors for a series of FLAG-TET2 fragments. Cell lysates were subjected to IP with FLAG antibody, followed by WB. CD, cysteine-rich dioxygenase domain.

(legend continued on next page)

comprise the largest family of E3s, form multiple cullin-ring ubiquitin ligase (CRLs) complexes that include a small RING protein, ROC1 or ROC2 (also known as RBX), which activates E2, and substrate recognition subunits. CUL4, conserved from yeast to humans, has two paralogs in mammalian cells, CUL4A and CUL4B. Both use damaged DNA binding protein 1 (DDB1) as a linker to interact with multiple *D*DB1-binding *WD*40 (DWD, also known as DCAF for *D*DB1 and *c*ullin-*a*ssociated *f*actors) proteins that serve as substrate recognition subunits. The functions of CUL4 genes have been genetically linked to chromatin regulation (Jackson and Xiong, 2009). This report shows that VprBP/DCAF1, one of the strongest and most abundant binding partners of DDB1 (McCall et al., 2008), promotes monoubiquitylation of TET enzymes and their DNA binding ability.

RESULTS

VprBP Binds the Cysteine-Rich Dioxygenase Domain of TET

The C-terminal WD40 domain of VprBP binds to DDB1 and, through DDB1, interacts with CUL4 to assemble an active catalytic moiety, while the N-terminal region is predicted to interact with substrates (McCall et al., 2008; Nakagawa et al., 2013). Thus, we established 293T cells stably expressing a FLAG-tagged VprBP deletion mutant that contains the N-terminal 909 amino acids (VprBP^{N909}). We conducted an immunoprecipitation (IP) followed by mass spectrometric (IP-mass spec) analysis in this cell line to identify proteins that specifically bind to the VprBP^{N909} mutant (Figure 1A). The VprBP^{N909} mutant does not contain the DDB1 binding domain, and thus the association with CUL4 and the catalytic ROC1 RING finger subunit is disrupted, potentially trapping the binding of VprBP with its substrates. We identified a large number of potential VprBP-interacting proteins, including TET2 (see Figure S1 and Table S1 available online). Immunoblotting confirmed the retention of VprBP^{N909} in TET2 immunoprecipitates and also demonstrated that full-length VprBP binds to TET2 (Figures 1A and 1E). To determine the VprBP binding region in TET2, we constructed several deletion mutants and found the C-terminal *c*ysteine-rich *d*ioxygenase (CD) domain of TET2 (CD2) to be primarily responsible for binding to VprBP (Figure 1B). Consistent with the high conservation of CD domains among TET paralogs, all three TET CD domains and full-length TET proteins bound to VprBP in cells (Figures 1C and 1D). Catalytically inactive TET CDs also bound to VprBP (Figure 1C), suggesting that the catalytic activity is not involved in this binding. Importantly, endogenous TET proteins were readily detected in association with endogenous VprBP in mouse embryonic fibroblasts (MEFs), mouse embryonic stem cells (ESCs), and human monocytes (Figure 1E). An in vitro binding assay showed that VprBP, but not DDB1, directly binds to TET2-CD (Figure 1F). Together, these studies demonstrated that VprBP binds directly to all three TET proteins.

VprBP Function Is Important for Paternal DNA Hydroxymethylation and Zygotic Development

To determine the functional significance of VprBP-TET interaction, the effect of *VprBP* deletion on 5hmC level in MEF cells was examined. Because *Vprbp* is essential for mouse embryo development and cell growth, we used a conditional *Vprbp* knockout mouse strain we previously created (McCall et al., 2008): *VprBP^{f}*. Here, expression of cre recombinase deletes a 2,358 bp genomic segment containing exons 7 and 8, which encodes 203 amino acid residues (residues Val172 to Ala374). *VprBP$^{f/f}$* MEFs were infected with adenovirus-expressing Cre to effectively delete *VprBP* gene and abolish the expression of *VprBP* mRNA, but not affecting the expression of either Tet2 or Tet3 (Figure 2A). Deletion of VprBP gene caused substantial reduction of 5hmC, suggesting that the function of VprBP is important for TET activity (Figure 2A).

One critical function of TET family dioxygenases is TET3-catalyzed paternal genome hydroxymethylation in the zygote (Gu et al., 2011). To determine the physiological significance of CRL4^{VprBP}-mediated TET activation, we next examined the role of VprBP in paternal genome DNA hydroxymethylation and zygotic development. *Vprbp$^{f/f}$* were crossed with *Zp3*-Cre mice expressing the cre recombinase under the promoter of mouse zona pellucida 3 gene (*Zp3*). This cross led to *Vprbp* knockout exclusively in the growing oocyte, prior to completion of the first meiotic division (Lewandoski et al., 1997). To determine the effects of oocyte *Vprbp* deletion on zygotic development, female *Vprbp$^{f/f}$* and *Vprbp$^{f/f}$;Zp3-Cre* mice were superovulated, and embryos were examined microscopically. While the *Vprbp$^{f/f}$* embryos developed to the four-cell stage, the *Vprbp$^{f/f}$;Zp3-Cre* zygotes were arrested at the one-cell stage and failed to start embryogenesis or cleavage (Figure 2B), which reveals a critical function of VprBP in zygotic development. Synchronously, VprBP was expressed at a readily detectable level in oocytes with an evident accumulation in the nucleus (Figure 2C). Efficient deletion of *VprBP* by *Zp3*-driven Cre was confirmed by immunohistochemistry (Figure 2C). This analysis showed a reproducible and partially penetrant developmental defect in a fraction of oocytes (Figures 2C and S2). Notably, deletion of *VprBP* in zygotes resulted in markedly reduced TET3 protein (Figure 2D) and a concomitant loss of paternal DNA hydroxymethylation (Figure 2E). Deletion of *VprBP* did not affect *Tet3* mRNA level (Figure 2F). These data demonstrate a critical function of VprBP in maintaining the level of Tet3 protein and supporting the activity of Tet enzymes during zygotic development. Zygotic deletion of Tet3 in mice, while abolishing 5mC-to-5hmC conversion in the male pronucleus, did not significantly affect early zygotic

(C) FLAG-tagged mouse TET CD domains were immunoprecipitated from 293T cells, and their associated proteins were detected by WB. CD1, CD2, and CD3 refer to the CD domain of mouse TET1 (residues 1,400–2,039, NP_001240786.1), TET2 (residues 1,042–1,912, NP_081660.1), and TET3 (residues 697–1,668, NP_898961.2), respectively. CM, catalytic mutant (H1620Y/D1622A for mouse TET1, H1295Y/D1297A for mouse TET2).
(D) FLAG-TET proteins were immunoprecipitated from 293T cells, and their associated proteins were detected by WB.
(E) Endogenous VprBP was immunoprecipitated from MEF, mouse ESCs, and human monocytes, and its association with TET proteins was determined by WB.
(F) Recombinant FLAG-TET2-CD was incubated with recombinant His_6-VprBP or GST-DDB1. Binding was monitored by WB.
See also Figure S1, Table S1, and Table S2.

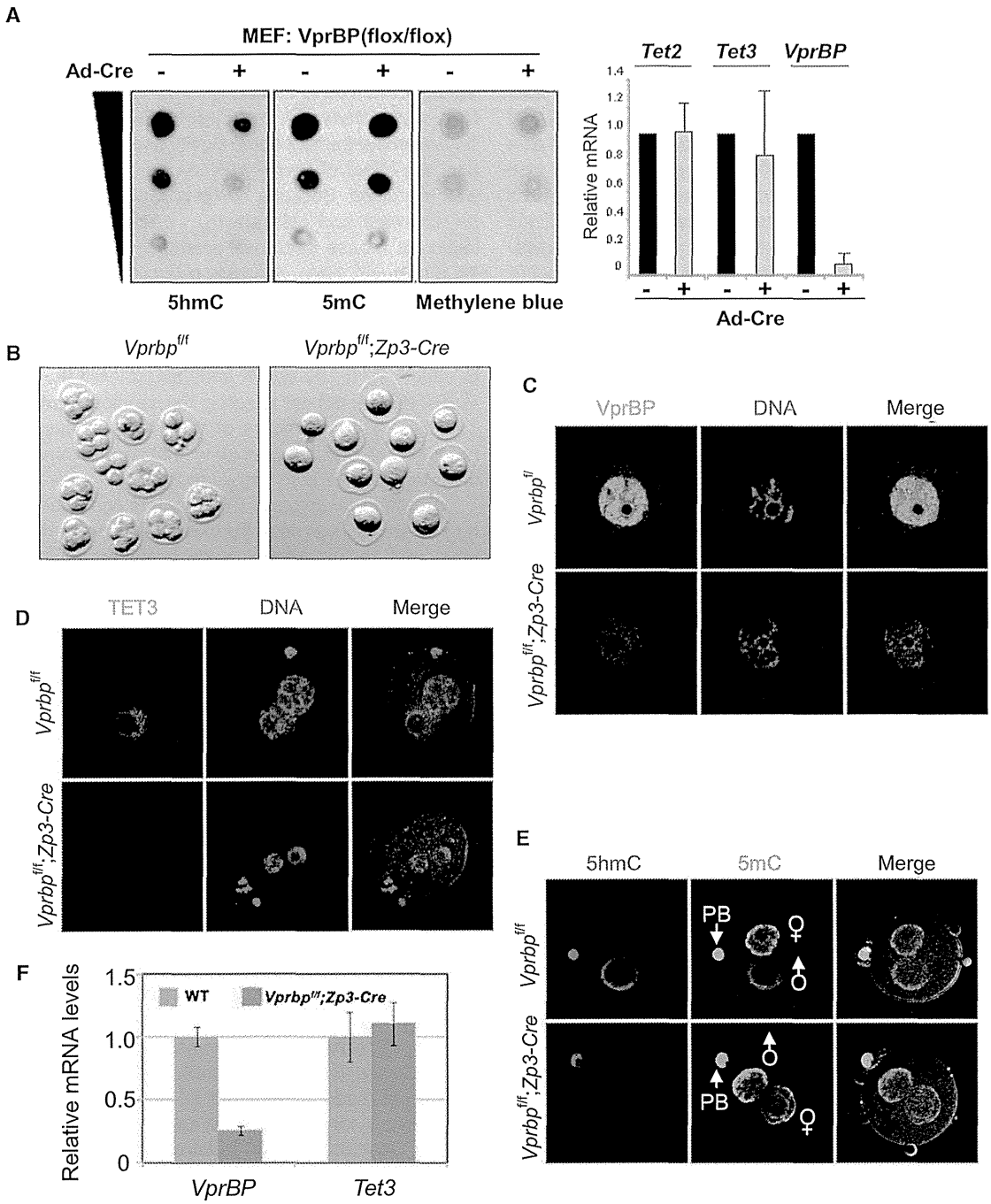

Figure 2. VprBP Is Essential for TET Activity

(A) *VprBP*$^{f/f}$ MEFs were infected with adenovirus expressing Cre. mRNA level was analyzed by quantitative RT-PCR, and 5mC and 5hmC level was analyzed by dot blot. Mean values ± SD of triplicates are presented.

(B) Female *Vprbp*$^{f/f}$ and *Vprbp*$^{f/f}$;*Zp3-Cre* mice were superovulated with PMSG and hCG before mating to wild-type males. Successful mating was confirmed by the presence of vaginal plugs. Forty-eight hours after hCG, embryos were obtained from the oviducts and examined microscopically.

(C) The expression of VprBP in *VprBP*$^{f/f}$ or *VprBP*$^{f/f}$;*Zp3-Cre* oocytes from the germinal vesicle (GV) stage was examined by immunofluorescence.

(D and E) The expression of Tet3 (B), 5mC, and 5hmC (C) in *VprBP*$^{f/f}$ or *VprBP*$^{f/f}$;*Zp3-Cre* oocyte-derived zygotes was examined by immunofluorescence.

(F) The expression of *VprBP* and *Tet3* mRNA in *VprBP*$^{f/f}$ or *VprBP*$^{f/f}$;*Zp3-Cre* oocytes from germinal vesicle (GV) stage was determined by quantitative RT-PCR analysis. Mean values ± SD of triplicates are presented.

See also Figure S2 and Tables S2 and S3.

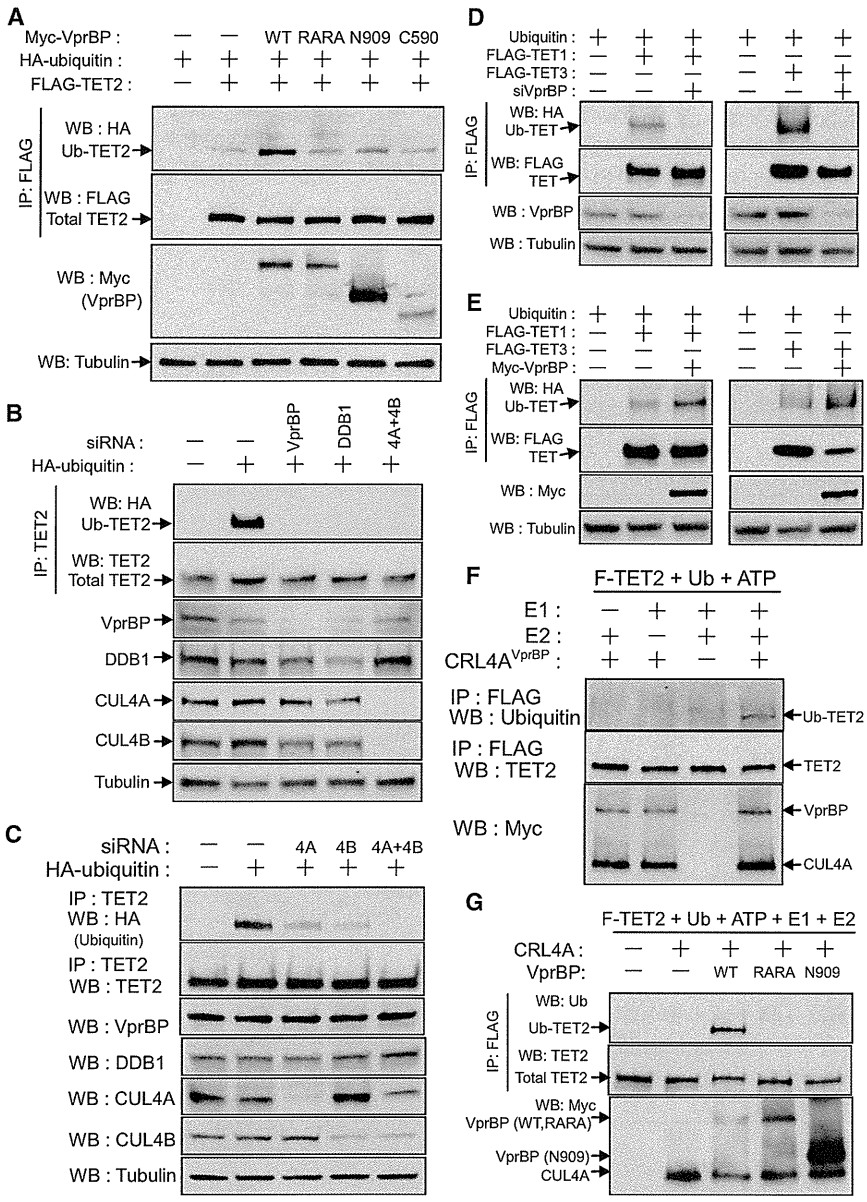

Figure 3. CRL4^{VprBP} Monoubiquitylates TET Proteins

(A) 293T cells transfected with plasmids of Myc-VprBP, FLAG-TET2, and HA-ubiquitin were lysed and subjected to IP with an antibody to FLAG under denaturing conditions (0.1% SDS). The resulting precipitates were blotted with the indicated antibodies.

(B) 293T cells were transfected with plasmids of HA-ubiquitin along with siRNA for VprBP, DDB1, or CUL4 and subsequently lysed and subjected to IP with an antibody to TET2 under denaturing conditions. Precipitates were immunoblotted.

(C) 293T cells transfected with a plasmid of HA-ubiquitin along with siRNA for CUL4A, CUL4B or CUL4A and CUL4B were lysed and subjected to IP with an antibody to TET2 under denaturing conditions. Precipitates were blotted.

(D) In vivo ubiquitylations of ectopically expressed TET1 and TET3 proteins were determined in cells transfected with siRNA targeting VprBP.

(E) In vivo ubiquitylations of ectopically expressed TET1 and TET3 proteins were determined in cells with or without coexpression of VprBP.

(F) Recombinant FLAG-TET2 was incubated with different combinations of E1, E2, and CRL4A^{VprBP} (E3) along with ATP and ubiquitin, followed by IP with a FLAG antibody. Ubiquitylated TET2 was examined by WB with anti-ubiquitin.

(G) Recombinant FLAG-TET2 was incubated with ubiquitin, E1, E2, and CRL4A along with different combinations of VprBP mutants, followed by IP with a FLAG antibody.

See also Figure S3 and Table S2.

development (Gu et al., 2011; Wossidlo et al., 2011), suggesting that developmental defects observed in *VprBP*-deficient zygotes involve additional events independent of the defect in paternal chromosome demethylation. Consistent with this notion, we noticed in the *VprBP*-deficient zygotes that pronuclei appeared and DNA was more condensed when compared to controls. It is likely that VprBP may have an additional substrate(s) that is important for cell-cycle progression in zygotes.

CRL4^{VprBP} Monoubiquitylates TET Proteins

To gain mechanistic insight into VprBP-TET interaction, we first carried out an in vivo ubiquitylation assay in cultured cells. This experiment revealed surprisingly that TET2 is ubiquitylated as a discrete band, which is indicative of monoubiquitylation, rather than a ladder of high-molecular weight conjugates that result from polyubiquitylation (Figure 3A). TET2 ubiquitylation was enhanced by the overexpression of wild-type VprBP, but neither VprBP^{RARA} (Figure S3A) mutant defective in DDB1 binding, VprBP^{N909} mutant lacking the DDB1-binding WD40 domain, nor VprBP^{C590} lacking the N-terminal portion involved in TET2 binding (Figure 3A). To directly test the possibility that TET2 is a substrate of CRL4^{VprBP}, we performed an in vivo ubiquitylation assay of TET2 in cells depleted for VprBP, DDB1, or a combination of CUL4A and CUL4B, which revealed markedly reduced monoubiquitylation of TET2 after knocking down each individual CRL4 component (Figure 3B). The decrease of TET2 monoubiquitylation by VprBP depletion was restored by ectopic expression of a siRNA-resistant VprBP (Figure S3B), confirming the specificity of VprBP knockdown on TET2 ubiquitylation. CUL4A and CUL4B, although closely related, are distinct in their subcellular localization. Whereas CUL4A resides predominantly in the cytoplasm, CUL4B localizes mostly in the nucleus (Nakagawa and Xiong, 2011). To determine the subcellular location of CRL4^{VprBP}-mediated ubiquitylation of TET2, we knocked down CUL4A and CUL4B separately and examined TET2 ubiquitylation. Monoubiquitylation of TET2 was substantially reduced to a similar level by

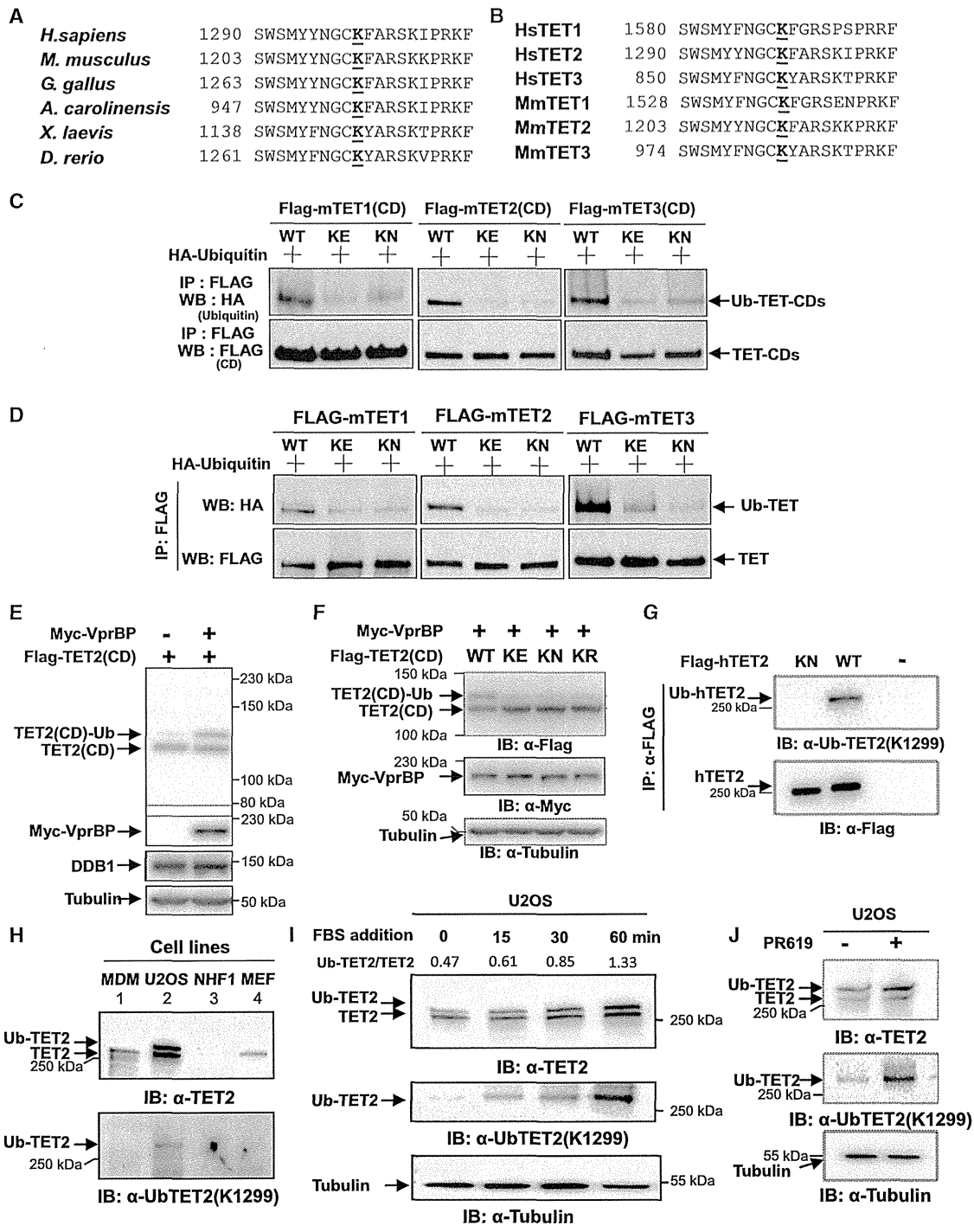

Figure 4. CRL4^{VprBP} Ubiquitylates TET Proteins on a Conserved Lys Residue

(A) Sequence alignment of TET2 surrounding K1299 from various vertebrate species, including human (*H. sapiens*, NCBI reference number NP_001120680.1), mouse (*M. musculus*, NP_001035490), chicken (*G. gallus*, NP_001264723), lizard (*A. carolinensis*, XP_003226445.1), frog (*X. laevis*, ADU77105), and zebrafish (*D. rerio*, XP_005168673).

(B) Sequence alignment of the human and mouse TET proteins surrounding human TET2-K1299, including human TET1 (NP_085128.2), TET2 (NP_001120680.1), TET3 (NP_659430.1), mouse TET1 (NP_081660), TET2 (NP_001035490.2), and TET3 (ADR57138.1).

(C and D) Ubiquitylation of the CD domain (C) and full-length (D) mouse TET proteins were determined in 293T cells transfected with plasmids expressing HA-ubiquitin, WT TET2, AML-derived K1299 mutant TET2, or the corresponding AML-derived TET1 and TET3 mutants. Cells were lysed and subjected to IP with a FLAG antibody under denaturing conditions. Precipitates were blotted.

(legend continued on next page)

the depletion of either *CUL4* gene and nearly completely abolished by the combined knockdown of both CUL4 genes (Figure 3C). This result suggests that TET2 can be ubiquitylated in both the cytoplasm and the nucleus and that both CUL4A and CUL4B participate in TET2 monoubiquitylation. Nearly complete elimination of TET2 monoubiquitylation by combined CUL4A and CUL4B knockdown also indicated that $CRL4^{VprBP}$ is the major ubiquitin ligase for TET2.

To determine whether TET1 and TET3 are also monoubiquitylated by $CRL4A/B^{VprBP}$, we knocked down VprBP and examined their ubiquitylation. We found that ectopically expressed TET1 and TET3 are both ubiquitylated as a discrete band which was almost completely abolished by VprBP knockdown (Figure 3D). Conversely, we coexpressed VprBP with either TET1 or TET3 and found a positive correlation between VprBP level and ubiquitylation level of TET1 and TET3 (Figure 3E). Together, these results demonstrate that $CRL4A/B^{VprBP}$ catalyzes monoubiquitylation of all three TET proteins.

We then carried out an in vitro ubiquitylation assay of TET2 and TET3. Incubation of immunopurified TET2 (Figure 3F) or TET3 (Figure S3C) with E1, E2, ubiquitin, ATP, and $CRL4A^{VprBP}$ E3 immunocomplex resulted in a clear, single, ubiquitylated species of TET2 and TET3 that was not seen when E1, E2, or E3 was omitted. In vitro incubation of purified TET2 (Figure 3G) or TET3 (Figure S3D) with a $CRL4A^{VprBP}$ immunocomplex containing mutant VprBP that is deficient in binding to DDB1 ($VprBP^{RARA}$ and $VprBP^{N909}$) abolished the TET2 monoubiquitylation.

TET Proteins Are Monoubiquitylated by $CRL4^{VprBP}$ E3 Ligase at a Conserved Lys Residue

Unlike degradation-associated polyubiquitylation that does not generally modify a specific lysine residue, monoubiquitylation usually targets a specific lysine. The first attempt to identify the TET monoubiquitylation site by IP-mass spec analyses was not successful (data not shown). We then reasoned that, if $CRL4^{VprBP}$-mediated TET monoubiquitylation is important for TET function, mutation of the ubiquitylation site in TET2 would cause loss of function in a disease such as AML, in which *TET2* is frequently mutated. In addition to truncations and frameshifts by insertions or deletions, a large number of TET2 missense mutations (>250) have been reported in AML. Intriguingly, we found mutations of only two lysine residues in TET2: K1117 (Gelsi-Boyer et al., 2009; Rocquain et al., 2010) and K1299 (Delhommeau et al., 2009; Jankowska et al., 2009; Kosmider et al., 2009). These mutations were reported to be mutated in two (K1117-to-R) and three (K1299-to-N and K1299-to-E) AML patients, respectively. K1299, but not K1117, is highly conserved among vertebrates as well as TET protein paralogs (Figures 4A, 4B, and S4A). We recreated paralogous AML mutants corresponding to K1299 of human TET2 in mouse Tet2 (K1212N and K1212E), mouse Tet1 (K1537N and K1537E), and mouse Tet3 (K983N and K983E). Both K-to-N and K-to-E mutations of all three TET proteins significantly reduced their respective ubiquitylation, regardless of whether the CD domain (Figure 4C) or full-length TET proteins (Figure 4D) were assayed. We also characterized the K1299R mutant, which replaces the Lys with a similar positively charged Arg. This replacement also disrupted TET2 ubiquitylation (Figure S4B). A residual ubiquitylated TET was still seen, especially for TET3, when the ubiquitylation site was mutated, but its intensity was not affected by the overexpression of VprBP as was the wild-type TET3 (Figure S4C), suggesting that this conserved lysine residue is the predominant site of VprBP E3 ligase. We conclude that all three TET proteins are primarily monoubiquitylated by $CRL4^{VprBP}$ on a conserved lysine residues paralogous to K1299 in TET2.

To more definitively demonstrate the monoubiquitylated form of TET proteins as a discrete band, we considered the large size of TET proteins (2,136, 2,002, and 1,660 residues for human TET1, TET2, and TET3, respectively), which might cause comigration of both modified and unmodified forms. To this end, we first coexpressed a shorter CD domain of TET2 (Figure 1B) with VprBP to increase the monoubiquitylated fraction and resolved the lysate by a low-percentage (7%) SDS-PAGE. A clearly separated band was seen when TET2 (CD) was singularly expressed. The intensity of this band was 20.2% of that of the unmodified form and was increased to 41.7% after VprBP overexpression (Figure 4E), suggesting that a significant fraction of TET2 can be monoubiquitylated by VprBP. Furthermore, mutations of K1299 to either glutamic acid (KE), asparagine (KN), or arginine (KR) all eliminated this band (Figure 4F).

To examine the ubiquitylation of endogenous TET2 protein, we raised a rabbit polyclonal antibody using a branched human TET2 peptide as an antigen that conjugated the last three amino acid residues of ubiquitin (Arg-Gly-Gly) onto the K1299 residue (see Experimental Procedures for details). After clearing the antibody twice with excess unmodified peptides, we verified the specificity of the anti-UbTET2(K1299) antibody by dot blot (Figure S4D). The anti-UbTET2(K1299) antibody readily detected a band in cells ectopically expressing wild-type TET2, but no band in cells expressing K1299N mutant TET2 (Figure 4G), validating monoubiquitylation at K1299. We then examined a panel of cell lines for in vivo TET2 ubiquitylation by resolving total cell

(E) 293T cells were transfected with a plasmid expressing the FLAG-tagged human TET2 CD domain and Myc-VprBP as indicated. Total protein lysates were separated on a 7% SDS-PAGE and blotted.

(F) 293T cells were cotransfected with plasmids expressing Myc-VprBP and FLAG-tagged WT or mutant TET2 CD domains as indicated. Total protein lysates were separated on a 7% SDS-PAGE and blotted. KE, K1299E; KN, K1299N; KR, K1299R.

(G) 293T cells were transfected with plasmid expressing indicated WT or ubiquitylation site mutant (KN) human TET2 protein. Cells were lysed in SDS (1%) buffer, diluted 10-fold, and subjected to IP with FLAG beads under denaturing conditions. Precipitates were blotted with FLAG and UbTET2 (K1299) antibodies.

(H) Total protein extracts were prepared from indicated cell lines using a SDS (1%) lysis buffer and revolved through a gradient (4%–15%) SDS-PAGE, and blotted with either TET2 or UbTET2(K1299) antibody.

(I) U2OS cells were serum deprived for 24 hr followed by FBS stimulation according to the indicated time course. The cells were then lysed with 1% SDS buffer and blotted with TET2 and UbTET2(K1299) antibody. The relative amount of monoubiquitylated TET2 was determined by normalization to unmodified TET2.

(J) U2OS cells were treated with 8 μM PR619 for 24 hr, lysed with 1%SDS buffer, and blotted with TET2 and UbTET2(K1299) antibody.

See also Figure S4 and Table S2.

lysates through a gradient (4%–15%) SDS-PAGE to achieve better separation of high molecular proteins. Both the level of total TET2 protein and the intensity of the upper band varied significantly from cell line to cell line (Figure 4H). Immunoblotting of the same lysates with the anti-UbTET2(K1299) antibody detected a single band in U2OS cells that corresponds to the upper band in size, but not in other cell lines that do not express the upper band (lower panel of Figure 4H), confirming the upper band as the K1299-monoubiquitylated form of TET2. The upper band of TET2 was expressed at a low level in serum-starved U2OS cells and was stimulated following serum stimulation (Figure 4I). This pattern of the upper band matches perfectly with the band detected by the anti-UbTET2(K1299) antibody (middle panel of Figure 4I). Treatment of cells with PR-619, a nonspecific inhibitor of deubiquitylase, increased both the intensity of the upper band and the band detected by the anti-UbTET2(K1299) antibody (Figure 4J). Together, these results demonstrate that TET2 is monoubiquitylated by VprBP-mediated E3 ligase at Lys1299.

VprBP-Mediated Monoubiquitylation Promotes TET Binding to DNA In Vitro

In exploring the functional significance of VprBP-mediated TET monoubiquitylation, we examined several possibilities including the effect of monoubiquitylation on TET's binding to the substrate DNA. Binding of TET proteins to DNA exhibits a preference for DNA containing unmodified cytosine (Ko et al., 2013; Xu et al., 2012). Both wild-type and AML-derived K1299N (KN) and K1299E (KE) mutant TET2 proteins were expressed and immunopurified from 293T cells and incubated with double-stranded DNA oligonucleotides containing a single unmethylated or methylated CpG. Gel-shift assay showed that wild-type TET2 bound readily to the unmethylated DNA oligo, as expected. However, both the K1299N and K1299E mutations disrupted the binding (Figure 5A). Mutations targeting the monoubiquitylation site of TET1 and TET3 also disrupted their ability to bind DNA (Figure 5B). Coexpression of VprBP, which increases TET2 monoubiquitylation (Figures 3A and 4E), enhanced TET2 DNA binding (Figure 5C).

We next performed sequential immunopurifications after triple transfection of cells with FLAG-TET2, Myc-VprBP, and HA-Ub. We first used the FLAG antibody to purify the total TET2 protein and then the HA antibody to enrich for ubiquitylated TET2. This experiment demonstrated that, when similar amounts of TET2 proteins were incubated with DNA oligonucleotides, TET2 eluted from HA beads was enriched for monoubiquitylation and bound DNA much stronger than TET2 eluted from FLAG beads (Figure 5D). The quantification showed that when normalized to total (FLAG-tagged) TET2, this sequential IP enriched the ubiquitylated form of TET2 by 4.55-fold, which correlates with a 4.5-fold increase of TET2 binding to DNA. Conversely, we performed sequential immunopurification and immunodepletion experiments, using first the FLAG antibody to purify total TET2 proteins and then the HA antibody to deplete ubiquitylated TET2. Depletion substantially removed monoubiquitylated TET2 and, accordingly, decreased DNA binding activity (Figure 5E), supporting the notion that monoubiquitylation promotes TET binding to DNA in vitro.

VprBP-Mediated Monoubiquitylation Promotes TET Binding to DNA In Vivo

To corroborate the in vitro assay, the effect of VprBP-mediated monoubiquitylation on TET2's binding to DNA was determined in cells. ChIP-qPCR assays on multiple, previously identified TET target sites (Deplus et al., 2013) were performed which showed that wild-type, but not K1299N or K1299E mutant TET2, bound to its target genes (Figure 6A). Coexpression with wild-type, but not RARA or N909 mutant VprBP deficient in DDB1 binding, enhanced TET2 DNA binding (Figure 6B). These results support the critical importance of both K1299 and VprBP in promoting TET2 binding to DNA.

The distribution of monoubiquitylated and unmodified TET2 was then determined in cells. It was noted, by direct immunoblotting, that the anti-TET2 antibody predominantly detects one single band in the lysate prepared using a mild NP-40 (0.5%) lysis buffer which does not solubilize chromatin-bound proteins. Two clear bands appeared from lysate prepared using 1% SDS-lysis buffer and boiling, which efficiently solubilizes chromatin-associated proteins (Figure 6C). Immunoblotting using the anti-UbTET2(K1299) antibody detected one band in SDS-lysate, but not in NP40-lysate, that corresponds in size to the upper band detected by the TET2 antibody, further supporting the presence of K1299-ubiquitylated TET2 presents predominantly in the NP40-insoluble, nuclear fraction. To directly demonstrate that the monoubiquitylated TET2 binds to chromatin, we separated U2OS whole-cell extracts made from a nonionic detergent (0.1% Triton X-100) lysis buffer into six fractions and determined the distribution of TET2 by direct immunoblotting using anti-TET2 antibody (Figure 6D). We found that upper monoubiquitylated TET2 is present almost exclusively in the chromatin-enriched fraction (P3) and was hardly detectable in the cytosolic (S1, S2, and P2) or soluble nuclear fractions (S3). A very small amount of lower, unmodified TET2 was also detected in the chromatin fraction. The same assay was repeated using the lysate derived from U2OS cells overexpressing K1299N mutant TET2. It was found that the lower, unmodified band of $TET2^{K1299N}$, like that wild-type TET2, was not detected in the cytosolic (S1, S2, and P2), but unlike the wild-type TET2, the ubiquitylation-deficient $TET2^{K1299N}$ was not detected in the chromatin-enriched fraction (Figure 6E). Collectively, these results demonstrate that VprBP promotes TET2 protein binding to DNA and that this binding requires the monoubiquitylation at Lys1299.

Oncogenic TET2 Mutations Disrupt VprBP Regulation

To directly test whether monoubiquitylation is critical for TET function in vivo, the CD domain and full length of three murine TET proteins that harbor mutations at the ubiquitylation site—Tet1 (K1537N, K1537E), Tet2 (K1212N, K1212E), and Tet3 (K983N, K983E)—were ectopically expressed. TET activity was examined in vivo by immunofluorescence using 5hmC antibody. Both wild-type and mutant TET proteins were expressed at similar levels (Figure S5A), and mutation of the monoubiquitylation site did not disrupt binding between the TET proteins and VprBP (Figure S5B). Both K1212E and K1212N (corresponding to K1299E and K1299N in human TET2) mutations targeting the monoubiquitylation site in mouse Tet2 abolished Tet2's

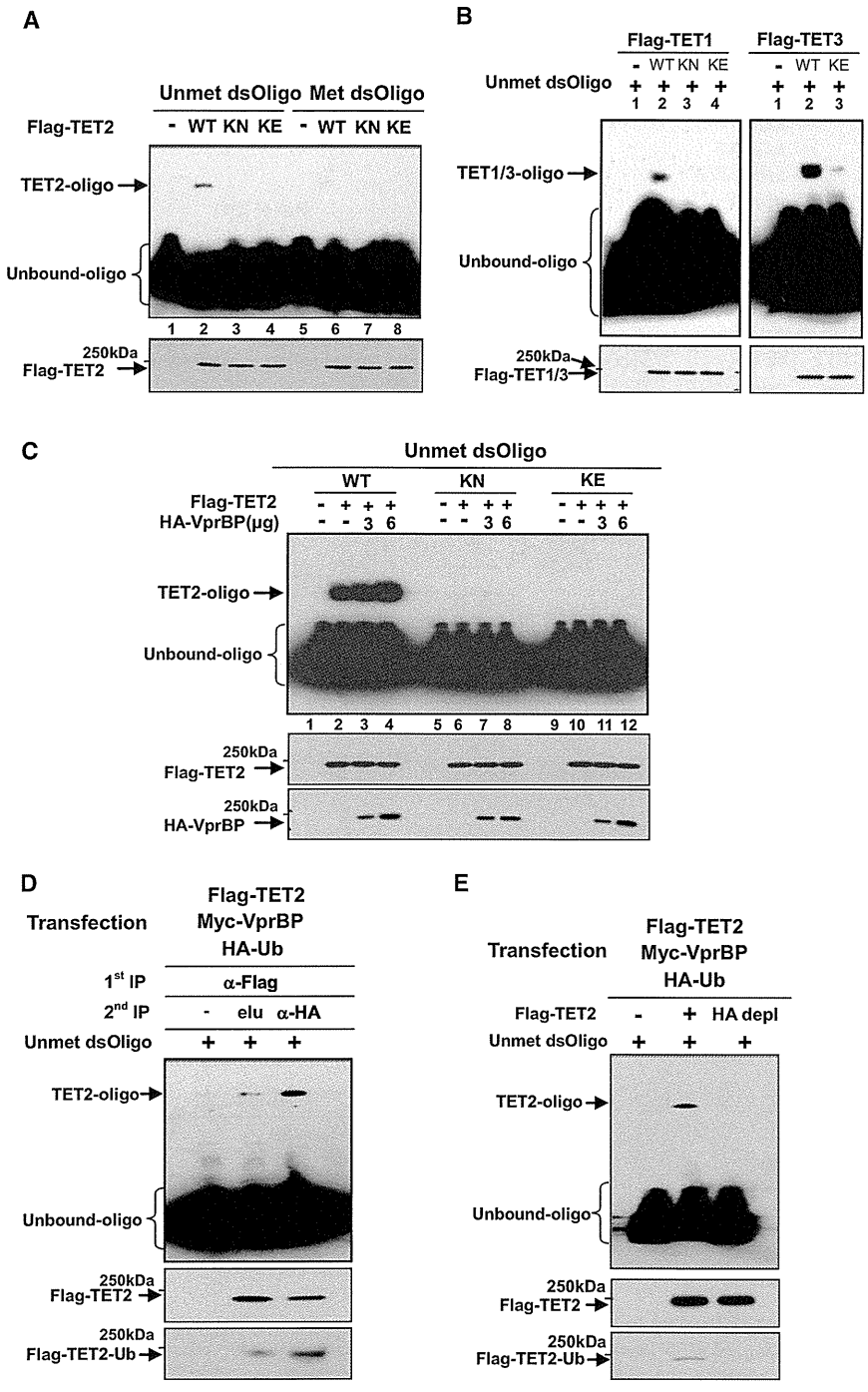

Figure 5. VprBP-Mediated Monoubiquitylation Promotes TET Binding to DNA In Vitro

(A) 293T cells were transfected with a plasmid expressing FLAG-tagged WT or AML-derived mutant TET2 as indicated. TET2 proteins were immunopurified and incubated with double-stranded DNA oligonucleotides containing a single unmethylated or methylated CpG. Protein-DNA binding was determined by gel-shift assay. Protein levels were analyzed by WB.

(B) 293T cells were transfected with a plasmid expressing FLAG-tagged WT or mutant TET1 or TET3 as indicated. Proteins were immunopurified from 293T cells and incubated with double-stranded DNA oligonucleotides containing a single unmethylated CpG. Protein-DNA binding was determined by gel-shift assay. Protein levels were analyzed by WB.

(C) 293T cells were transfected either alone with plasmids expressing FLAG-tagged WT or mutant TET2, or cotransfected with HA-VprBP as indicated. Proteins were immunopurified from 293T cells and incubated with DNA oligonucleotides containing a single unmethylated CpG. Protein-DNA binding was determined by gel-shift assay. Protein levels were analyzed by WB.

(D) 293T cells were triply transfected with FLAG-TET2, Myc-VprBP, and HA-Ub. Sequential immunopurification was performed, using first the antibody to FLAG to purify TET2 protein and then the antibody to HA to enrich ubiquitylated TET2. DNA binding activity of proteins eluted from FLAG beads or HA beads was determined by gel-shift assay. Protein and ubiquitylation levels were analyzed by WB.

(E) 293T cells were triply transfected with FLAG-TET2, Myc-VprBP, and HA-Ub. Immunopurification and immunodepletion were performed, using first the antibody to FLAG to purify TET2 protein and then the antibody to HA to deplete ubiquitylated TET2. DNA binding activity of proteins before or after HA depletion was determined by gel-shift assay. Protein and ubiquitylation levels were analyzed by WB.

See also Table S2.

activity in catalyzing 5hmC production in cells, whether assayed using full-length protein (Figure 7A) or CD domain (Figure S5C). Dot-blot assay using the genomic DNA isolated from transfected cells confirms that both K1212E and K1212N mutants failed to produce 5hmC in vivo (Figure S5D), which also applied to both Tet1 and Tet3. Regardless of assaying using the full length and CD domain, mutations targeting the monoubiquitylation site in either Tet1 (Figure S5E) or Tet3 (Figure S5F) also abolished the function of these two Tet enzymes in producing 5hmC in cells under immunofluorescence. Dot-blot assay of genomic DNA further confirmed the loss of activity in producing 5hmC in cells by both mutant Tet1 and Tet3 with disrupted monoubiquitylation site (Figure S5D). These results indicate that VprBP binding to TET proteins per se is not sufficient for TET activity, but rather that monoubiquitylation is critical for TET activity (see Discussion). Mutation of Lys983 to either Glu (K983E) or Asn (K983N) in both the CD domain and full-length Tet3, but not in Tet1 or Tet2, also altered Tet3's almost exclusive nuclear localization to one that is mostly cytoplasmic. Whether monoubiquitylation selectively regulates the subcellular localization of TET3 has not been determined.

TET2 gene is frequently mutated in hematopoietic malignancies. More than half of the mutations result in protein

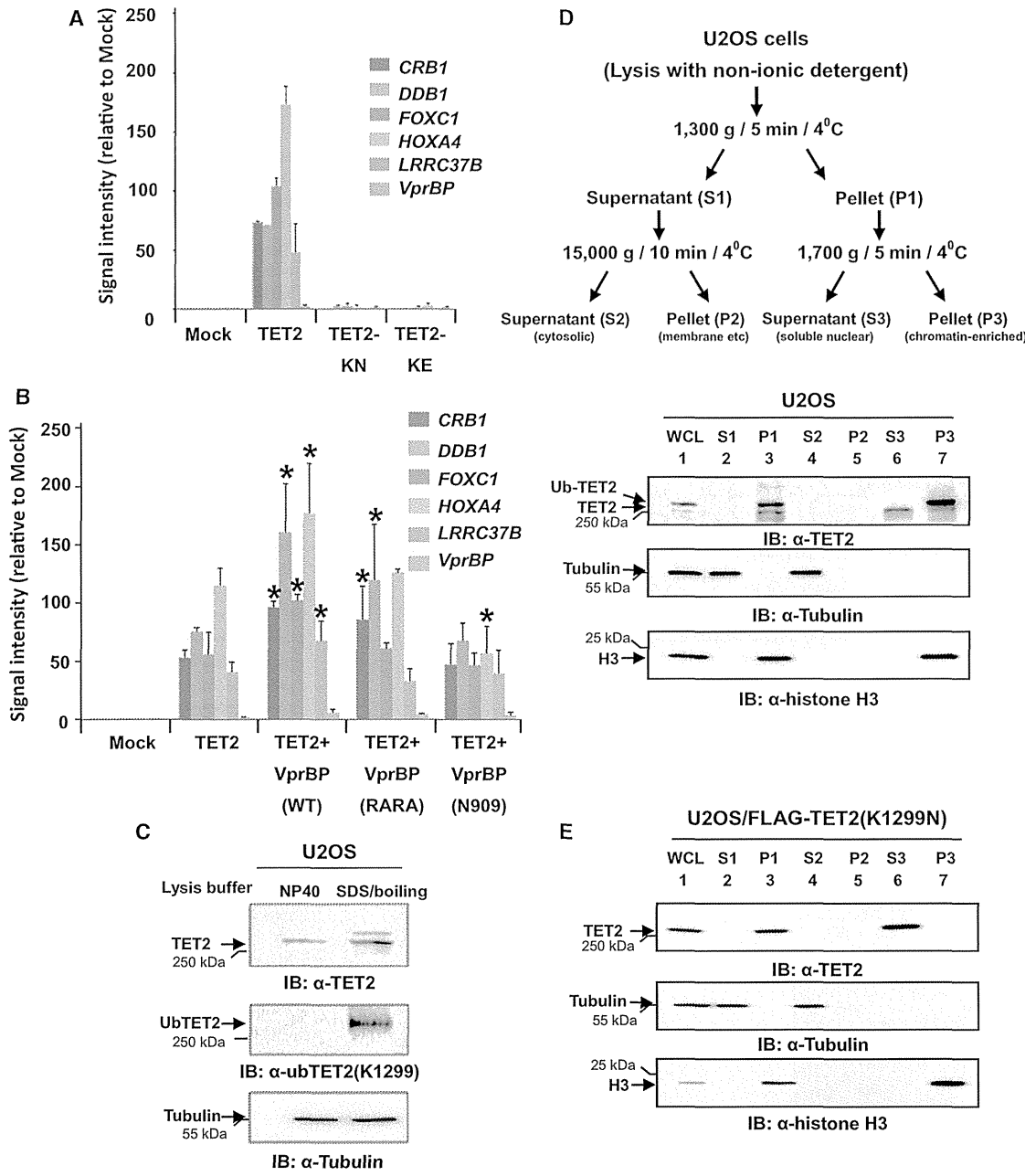

Figure 6. VprBP-Mediated Monoubiquitylation Promotes TET Binding to DNA In Vivo

(A) 293T cells were transfected with plasmid DNA encoding FLAG-tagged WT or lysine mutants of TET2. DNA/protein complexes were crosslinked and subjected to ChIP analysis with a FLAG antibody. Immunoprecipitates were analyzed by quantitative PCR (qPCR) with primers for the indicated TET2 target gene promoters. The signal intensity on the y axes represents the fold enrichment of DNA amplified by qPCR from cells expressing TET2 compared with that from mock cells transfected with empty vector. See Table S4 for primer sequences. Mean values ± SD of triplicates are presented.

(B) 293T cells were transfected with plasmid DNAs expressing FLAG-tagged TET2 and WT or mutant VprBP proteins as indicated. ChIP-qPCR analyses were performed as in Figure 6A. The signal intensity on the y axes represents the fold enrichment of DNA amplified by qPCR from cells expressing TET2 compared with that from mock cells transfected with empty vector. See Table S4 for primer sequences. Mean values ± SD of triplicates are presented.

(C) U2OS cells were lysed with 0.5% NP40 or 1% SDS buffer, followed by WB with TET2 and UbTET2(K1299) antibody, respectively.

(D) U2OS cells were lysed in a non-ionic (0.1% Triton X-100) lysis buffer, and lysates were separated into six fractions, followed by WB.

(E) U2OS cells were transfected with a plasmid expressing K1299N mutant TET2 and then lysed, fractionated, and blotted as in Figure 6D.

See also Tables S2 and S4.

truncation, indicating that loss of function is responsible for pathogenesis. In addition, several hundred nonsynonymous point mutations have been reported, but only a few that disrupt the binding of TET2 with either α-KG or Fe^{2+} have been functionally characterized (Ko et al., 2010). Given our finding that two different AML mutations targeting the K1299 monoubiquitylation site of TET2 inactivate its activity in vivo, we hypothesized that an additional mutation(s) may disrupt both $CRL4^{VprBP}$-mediated TET2 monoubiquitylation and TET2 activity. A number of AML-derived point mutations surrounding K1299 at the homologous site in mouse Tet2 were created, and their ubiquitylation was determined. Several mutations, in addition to K1299N and K1299E, were found to abolish Tet2 ubiquitylation, including C1298Y, F1300S, and R1302G (corresponding to C1211Y, F1213S, and R1215G in mouse Tet2) (Figure 7B), which has been reported in three, two, and two independent cases of human AML, respectively. Binding analysis revealed that F1213S and R1215G disrupted TET2 binding to VprBP (Figure 7C), providing an explanation of how mutations targeting these two residues disrupt TET2's monoubiquitylation. However, the C1211Y mutation did not disrupt the monoubiquitylation site nor significantly affect VprBP-TET2 binding, suggesting an additional step after binding of VprBP to TET2 that is important for $CRL4^{VprBP}$-mediated TET2 monoubiquitylation. Similar to the K1299N and K1299E mutants, ubiquitylation-deficient C1211Y, F1213S, and R1215G mutants all lost their activity in vivo (Figure 7D). In vitro assay using two different substrates, methylated double-stranded DNA (dsDNA) oligonucleotides (Figure S5G), and total genomic DNA (Figure S5H) demonstrated that mutants of TET2 deficient in monoubiquitylation still retain the catalytic activity as determined by the decrease of 5mC and accumulation of 5caC. Together, these results demonstrate that multiple, recurrent AML-derived mutations in TET2 disrupt $CRL4^{VprBP}$-mediated TET2 monoubiquitylation, while not affecting TET2's catalytic activity, and disrupt the VprBP-TET2 binding, the monoubiquitylation site, or another undetermined regulatory step, leading to functional inactivation of TET2 in vivo (Figure 7E).

DISCUSSION

VprBP Is a Critical Regulator of TET Family Dioxygenases

While the biological function and biochemical mechanism of TET enzymes have been extensively investigated, little is known about their regulation at present. We have shown that VprBP is a critical regulator of all three TET enzymes. The importance of VprBP in promoting the function of TET is supported by the genetic evidence that conditional knockout of *Vprbp* in oocytes resulted in a loss of TET3 and abolishment of paternal chromosome 5hmC. VprBP's importance is also supported by the finding that, in leukemia, multiple recurrent oncogenic mutations in TET2 disrupt VprBP-mediated TET2 activation.

$CRL4^{VprBP}$-Mediated Monoubiquitylation Promotes TET Binding to DNA

We present compelling evidence in this study that VprBP targets the TET proteins for monoubiquitylation by the $CRL4^{VprBP}$ E3 ligase. A lysine residue (K1299 in human TET2), which is invariably conserved among all three TET proteins, is identified as the site of $CRL4^{VprBP}$-mediated monoubiquitylation. Mutation of this conserved lysine residue abolishes the monoubiquitylation of all three TET proteins. We demonstrated in vivo TET2 monoubiquitylation using the antibody specifically recognizing K1299-ubiquitylated TET2. The abundances of the monoubiquitylated TET2 vary from cell line to cell line, are inhibited by a deubiquitinase inhibitor, and are increased when cells are stimulated to enter the cell cycle or when VprBP is overexpressed. These observations indicate that TET2 monoubiquitylation is dynamically regulated in cells.

VprBP-mediated monoubiquitylation plays a critical role in TET activation by promoting their ability to bind DNA, but not catalytic activity of TET enzyme. As binding to DNA is a prerequisite for the function of TET in catalyzing 5mC hydroxylation, our findings provide a molecular basis for the activation of TET dioxygenases by VprBP-mediated monoubiquitylation. The exact mechanism by which monoubiquitylation promotes TET DNA binding is currently unknown. It is conceivable that conjugation of a ubiquitin could disassociate TET from a factor that blocks TET's binding to DNA, bridge the binding of TET with a factor that recruits TET to DNA, or expose a masked DNA binding domain. Very recently, the crystal structure of a fragment of human TET2 (residues 1,129–1,936) which deleted a large low-complexity region (residues 1,481–1,843) predicted to be unstructured has been resolved in complex with DNA (Hu et al., 2013). Notably, in this TET2-DNA complex, the K1299 monoubiquitylation site directly contacts DNA. We speculate that monoubiquitylation in TET may directly affect its binding with DNA, for example by stabilizing the conformation of full-length TET2 containing the unstructured sequence.

Oncogenic Mutations in TET2 Disrupt VprBP-Mediated Regulation

The *TET2* gene is frequently mutated in hematopoietic malignancies of both myeloid and lymphoid lineages. The results presented in this study reveal a mechanism for oncogenic inactivation of TET2, by disruption of VprBP-mediated monoubiquitylation. As we selectively characterized only a small number of point mutations surrounding the ubiquitylation site, the full spectrum of oncogenic mutations targeting VprBP-mediated TET2 ubiquitylation is unknown and could be underappreciated. *TET* genes are not frequently mutated in solid tumors. Yet, many different types of malignant tissues have been found to contain very low or undetectable levels of 5hmC compared with normal tissues (e.g., Yang et al., 2013), implicating additional mechanisms for functionally inactivating TET. In glioma where mutation of a *TET* gene has not been reported, TET enzymes are catalytically inactivated by the D-2-HG oncometabolite produced by mutated IDH1 (Chowdhury et al., 2011; Dang et al., 2009; Xu et al., 2011). The findings reported here present an additional target, $CRL4^{VprBP}$ E3 ligase, for oncogenic inactivation of TET function. It will be important to explore the expression of VprBP and other CRL4 components in different types of tumors.

EXPERIMENTAL PROCEDURES

More detailed descriptions for procedures below and additional procedures are provided in the Supplemental Information.

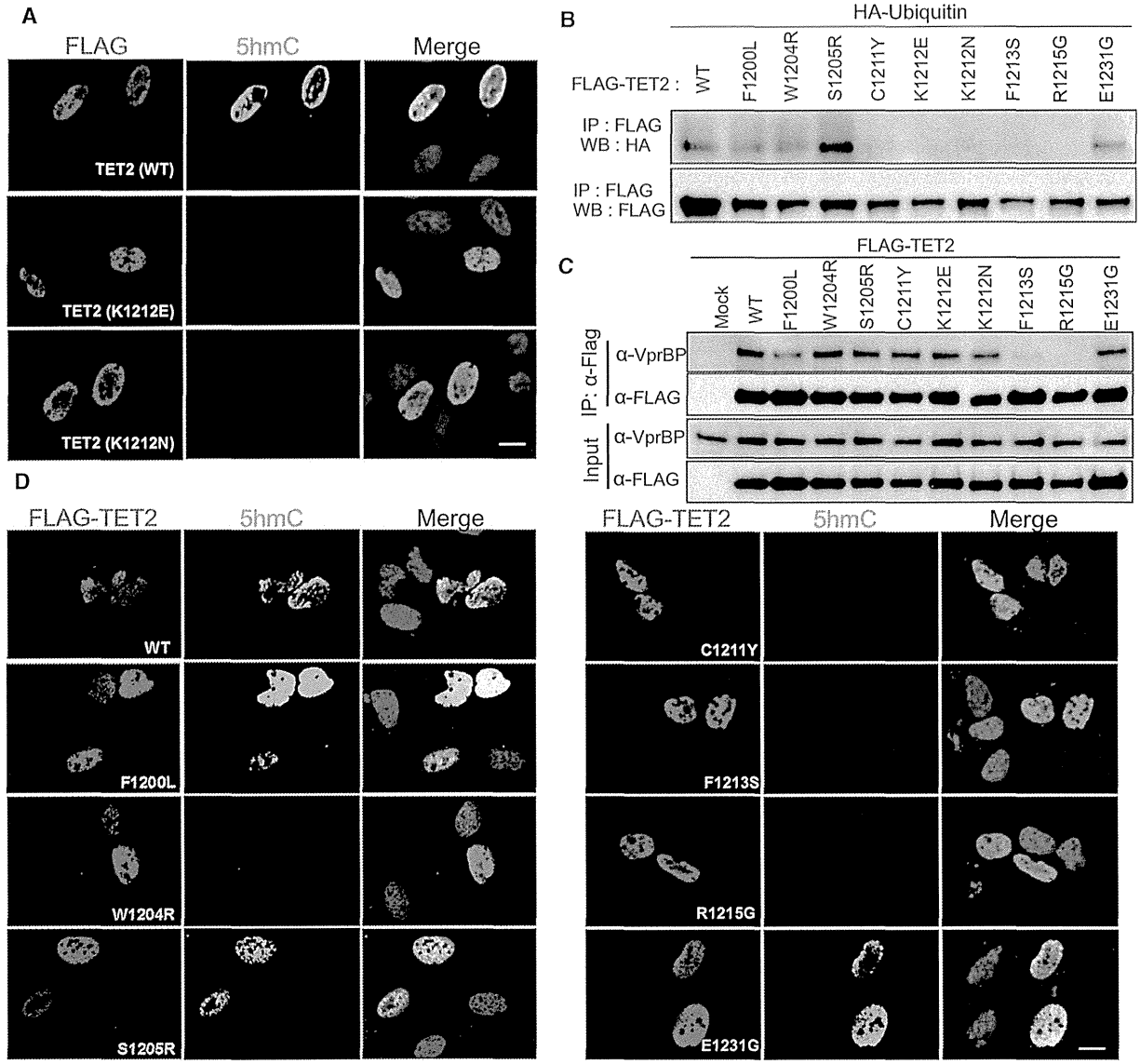

E

Mutations in leukemia	Murine counterpart	VprBP binding	Ubiquitylation	In vivo Activity	In vitro Activity
F1287L	F1200L	√	√	√	√
W1291R	W1204R	√	√	X	√
S1292R	S1205R	√	√	√	√
C1298Y	C1211Y	√	X	X	√
K1299E	K1212E	√	X	X	√
K1299N	K1212N	√	X	X	√
F1300S	F1213S	X	X	X	√
R1302G	R1215G	X	X	X	√
E1318G	E1231G	√	√	√	√

Figure 7. Multiple Recurrent Leukemia-Derived Mutations in TET2 Disrupt VprBP-Mediated TET2 Monoubiquitylation

(A) U2OS cells were transiently transfected with an expression vector for FLAG-TET2 or the TET2 lysine mutant, and the cells were fixed and immunostained with anti-FLAG (red) and anti-5hmC (green) antibodies. The nucleus was visualized by DAPI. Scale bar, 10 μm.

(B) The in vivo ubiquitylation level of TET2 leukemia mutants was examined by IP followed by WB.

(C) Binding of TET2 leukemia mutants to VprBP was examined by IP followed by WB.

(legend continued on next page)